ELSEVIER

Coordination Chemistry Reviews
216–217 (2001) 249–286

COORDINATION CHEMISTRY REVIEWS

www.elsevier.com/locate/ccr

Transition and post-transition metal systems incorporating linked synthetic macrocycles as structural elements

Jy D. Chartres [a], Leonard F. Lindoy [b,*], George V. Meehan [a]

[a] *School of Biomedical and Molecular Sciences, James Cook University, Townsville, Qld 4811, Australia*
[b] *Centre for Heavy Metal Research, School of Chemistry, University of Sydney, Sydney, NSW 2006, Australia*

Received 8 August 2000; accepted 9 January 2001

Contents

* Corresponding author. Tel.: +61-2-93514400; fax: +61-2-93517067.
E-mail address: lindoy@chem.usyd.edu.au (L.F. Lindoy).

PII: S0010-8545(01)00313-7

Abstract

The transition and post-transition metal chemistry of linked macrocyclic ligand systems incorporating all nitrogen as well as mixed-donor sets is reviewed.

Keywords: Macrocycle; Linked-macrocycles; Heavy-metal; Transition metal

1. Introduction

In this review, recent developments in the transition and post-transition ion chemistry of covalently linked macrocyclic ring systems are presented. The published literature in the area up to 1995–96 has already been reviewed recently by one of us [1,2] and the present work is, in part, an update of these prior discussions.

A major thrust in recent macrocyclic ligand research has been the development of multi-component structures in which individual macrocyclic units are joined together by either covalent bonds or, in a few instances, by weaker hydrogen bonding interactions. The present discussion is concerned with systems of the former type incorporating covalently linked rings. In theory, such systems are able to display a range of molecular structures that include, linear, branched, stacked, and dendritic arrangements of their macrocyclic components. The resulting nanometre-scale structures are normally capable of binding two or more metal ions simultaneously in defined positions relative to each other. Macrocyclic rings are desirable building blocks for incorporation in such systems since, because of the operation of the macrocyclic effect, they typically yield more kinetically and thermodynamically stable metal complexes than their open-chain analogues. Thus, the incorporation of macrocyclic rings will help maintain the corresponding metal derivative's integrity under a variety of conditions [3].

A considerable number of systems of the above type have involved crown or azacrown rings [4–6] — largely reflecting the ease of synthesis of suitably functionalised derivatives involving such macrocyclic types, although porphyrin-derived systems [7] have also been increasingly employed in this context. Metal complexes of 'mechanically' linked macrocycles of the catenane type have been reviewed elsewhere [8,9] and will not be discussed here. Beside their considerable intrinsic interest, linked di- or polynuclear macrocyclic complexes may serve as models for the charge transfer, electron transport and allosteric behaviour found in many metal-containing biochemical systems [10–12].

Further interest in systems of the above type has been generated by the observation that several linked macrocyclic derivatives, including selected dimetal derivatives, have been demonstrated to inhibit particular HIV strains with low levels of cytotoxcity [13–16].

2. Linked tri-aza ring systems

2.1. Bis-macrocyclic ligands

Since 1,4,7-triazacyclononane (tacn) was first incorporated into linked macrocyclic systems over two decades ago [17], the coordination chemistry of the resulting systems has received considerable attention [2]. Recent examples of such linked rings incorporate *o*-, *m*- and *p*-xylyl linkers to yield the series of bis(tacn) derivatives given by **1**; the crystal structure of the dinuclear Cu(II) complex $[Cu_2L(OH)_2](BPh_4)_2$, where L = **1b**, has been determined (Fig. 1) [18]. Each Cu(II) is coordinated to the face of a macrocycle, with the secondary nitrogens and two μ-hydroxo oxygens forming the base of a pseudo-square pyramid; the tertiary amine occupies an elongated axial position. A weak anti-ferromagnetic interaction occurs between the linked metal centres which are separated by 2.95 Å. Interestingly, the orientation of the aromatic linker is such that it is directed to one side of the CuO_2Cu plane, yielding a hydrophobic pocket over one of the bridging μ-hydroxo groups.

In another study, Spiccia and co-workers have also investigated the metal coordination of the xylyl-linked bis(tacn) systems **1** [19]. The X-ray structure of the di-Cu(II) complex $[Cu_2LBr_4]$, where L = **1a**, confirms that the two triamine rings

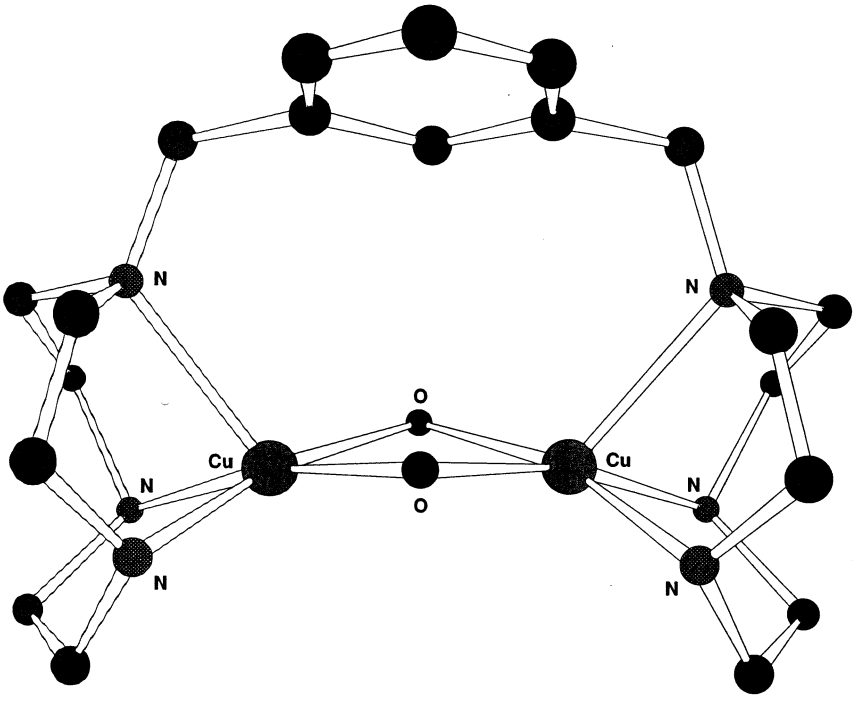

Fig. 1. The X-ray structure of the cation $[Cu_2L(OH)_2]^{2+}$ [L = **1b**] [18].

bind to different metal centres. Two secondary amines and two bromide ions form the base of a distorted square pyramidal coordination sphere for each metal ion, with a tertiary amine donor occupying the apical position in each case. The intermetallic distance is 7.21 Å and hence no metal–metal interaction is present.

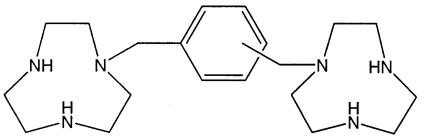

1a *ortho-*
1b *meta-*
1c *para-*

Using an alternative procedure, a Cu(II) complex of **1a** was synthesised employing a low metal ion:ligand ratio. Under these conditions a mononuclear product is formed. The X-ray structure (Fig. 2) of the product, $[CuL](ClO_4)_2$, where L = **1a**, reveals that the metal centre is sandwiched between two tri-aza rings belonging to the one ligand such that a Jahn–Teller distorted, octahedral coordination geometry

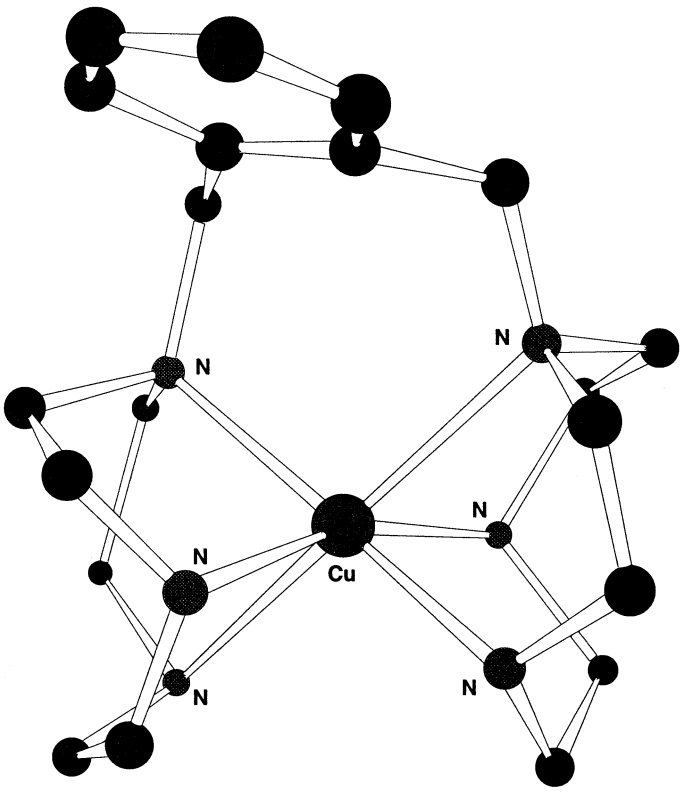

Fig. 2. The X-ray structure of the cation $[CuL]^{2+}$ [L = **1a**] [19].

results. The same mode of coordination is also exhibited in the X-ray structure of the corresponding mononuclear Ni(II) complex $[NiL](ClO_4)_2$. Unsuccessful attempts to isolate similar mononuclear complexes of **1b** or **1c** were attributed to the *m*- and *p*-xylyl linking groups preventing simultaneous coordination of both macrocyclic rings to a single Ni(II) centre. Instead, for L = **1c**, a linked di-Ni(II) complex $[Ni_2L(OH_2)_6](ClO_4)_4$ was formed containing *fac*-coordinated macrocyclic subunits, with water molecules completing a distorted octahedral coordination geometry around each metal centre. The metal centres are located on opposite sides of the plane of the ligand to yield an *anti* configuration, with the metal–metal distance being 11.68 Å.

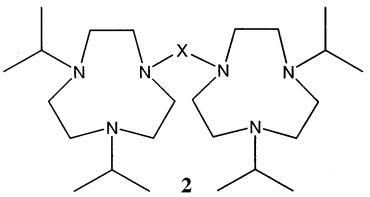

2

Sterically hindered variants of the bis(tacn) moiety have been used to model the binding of dioxygen to copper centres as occurs in certain metalloenzymes [20–22]. Reaction of **2** [X = $(CH_2)_2$, *m*-xylyl or *p*-xylyl] with the $[Cu(CH_3CN)_4]^+$ cation results in the isolation of air-sensitive di-Cu(I) complexes of type $[Cu_2L(CH_3CN)_2]^{2+}$ as their ClO_4^-, SbF_6^- or $CF_3SO_3^-$ salts [21]. A broad singlet at ca. 2.3 ppm in the ^{1}H-NMR spectra and a weak ν(C≡N) at ca. 2270 cm^{-1} in the FTIR spectra of these species strongly suggests that coordination of an acteonitrile ligand to each of the Cu(I) centres occurs. Treatment of $[Cu_2L(CH_3CN)_2](CF_3SO_3)_2$, where L = **2** (X = *m*-xylyl), with CO (1 atm) replaces the acetonitrile ligands with CO (ν_{CO} 2079 cm^{-1}). The structure of the latter product was confirmed by X-ray analysis (Fig. 3). The structure reveals the expected pseudo-tetrahedral geometry of the Cu(I) centres, composed of an N_3-donor macrocyclic set and a coordinated CO molecule. The *anti* conformation of the complex is reflected in a large metal–metal distance of 10.06 Å.

Low-temperature oxygenation of the ethyl-linked complex $[Cu_2L(CH_3CN)_2](ClO_4)_2$, where L = **2** [X = $(CH_2)_2$], leads exclusively to the formation of a corresponding bis(μ-oxo)dicopper adduct [22]. The X-ray structure of $[Cu_2L(\mu\text{-}O_2)](SbF_6)_2$, where L = **2** [X = $(CH_2)_2$] (Fig. 4), has been determined and is characterised by a 'short' Cu–Cu distance of 2.78 Å and an O···O distance of 2.35 Å, the latter confirming the cleavage of the dioxygen bond. Hydrogen bonding interactions (2.3–2.6 Å) between the bridging oxygens and the methine protons of the pendant *iso*-propyl groups are also observed. Warming of a CH_2Cl_2 solution of the complex results in oxidative cleavage of an *iso*-propyl substituent in a clean monooxygenase reaction to yield acetone. This *N*-dealkylation proceeds in quantitative yield, with no scission of the ethyl linker being observed. The observed regioselectivity is attributed to the inaccessibility of the ethyl linker hydrogens to the Cu_2O_2 core (in accordance with the situation in the solid state structure).

Relative to the above di-Cu(I) complex, alternative oxygen binding pathways arise when a xylyl-linker is substituted for ethyl in the ligand. Namely, such a change results in intermolecular binding being competitive with intramolecular

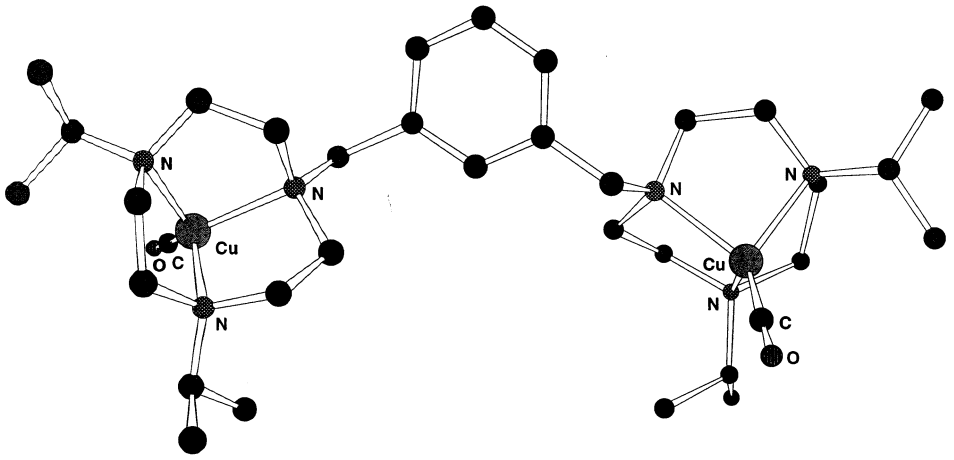

Fig. 3. The X-ray structure of the cation $[Cu_2L(CO)_2]^{2+}$ [L = **2** (X = *m*-xylyl)] [21].

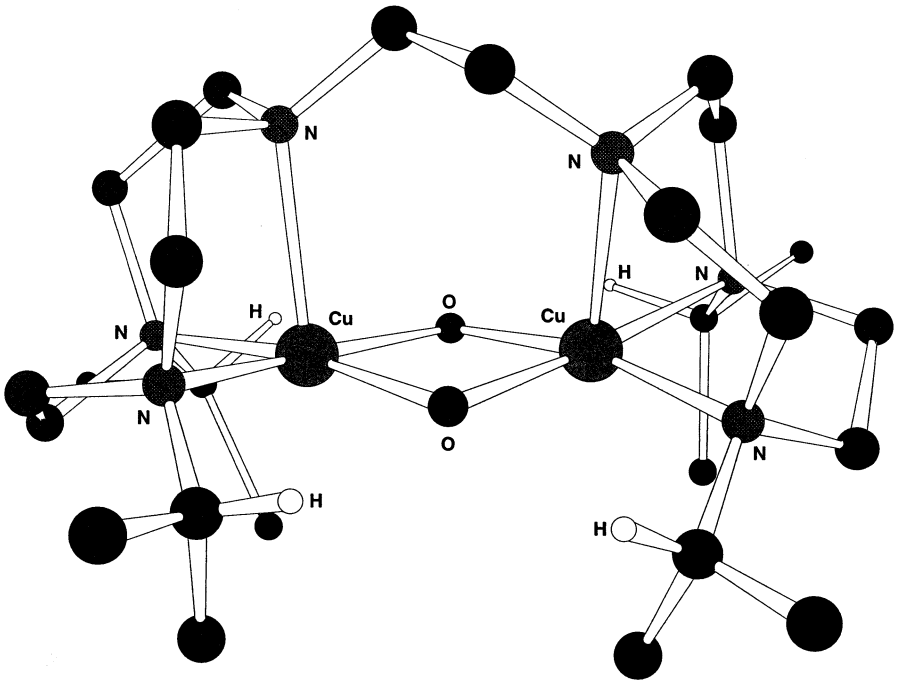

Fig. 4. The X-ray structure of the cation $[Cu_2L(\mu\text{-}O_2)]^{2+}$ {L = **2** [X = $(CH_2)_2$]} [22].

binding. At low concentrations of $[Cu_2L(CH_3CN)_2]^{2+}$, where L = **2** (X = *m*-xylyl), intramolecular oxygen binding appears to lead predominantly to a (μ-η^2:η^2-peroxo)dicopper species, $[Cu_2L(\mu\text{-}\eta^2\text{:}\eta^2\text{-}O_2)]^{2+}$, where L = **2** (X = *m*-xylyl). The latter differs from the $Cu_2(\mu\text{-}O_2)$ core described above in that the O–O bond remains intact. The formation of the (μ-η^2:η^2-peroxo)dicopper species appears to be a function of the longer metal–metal separation present in $[Cu_2L(CH_3CN)_2]^{2+}$, where L = **2** (X = *m*-xylyl). The μ-η^2:η^2-peroxo species was identified by its optical (λ_{max} at 366 nm; $\varepsilon \sim 20\ 000\ M^{-1}\ cm^{-1}$) and Raman [$\nu_{O-O} \sim 720$–$750\ cm^{-1}$; $\Delta\nu(^{18}O) = 42\ cm^{-1}$] spectra. However, at higher concentration, the major species identified was a (μ-oxo)dicopper species [λ_{max} at 320 nm and 430 nm; $\varepsilon \sim 20\ 000\ M^{-1}\ cm^{-1}$ and ν_{Cu-O} at 597 cm^{-1}; $\Delta\nu(^{18}O) = 24\ cm^{-1}$]. Mass spectrometry revealed that this species is in fact a 'dimer-of-dimers', incorporating intermolecular oxygen binding. In this complex of L = **2** (X = *p*-xylyl), the macrocylic compartments are now held far enough apart that intramolecular complex binding is precluded.

As a consequence of the disposition of the *m*-xylyl linker close to the (μ-η^2:η^2-peroxo)dicopper core (arising from the presence of intramolecular 'peroxo' binding), decomposition of the linker via an arene hydroxylation mechanism is promoted. The resulting (μ-phenoxy)(μ-hydroxo)dicopper(II) complex was recovered in 55% yield and was extensively characterised, including a preliminary X-ray structure determination. The product yielded a sharp ν(OH) at 3632 cm^{-1} in its FTIR spectrum and two absorptions at 680 and 380 nm ($\varepsilon \sim 3000\ M^{-1}\ cm^{-1}$) in its UV–vis spectrum. Of the latter, the first is an envelope of bands corresponding to Cu(II) d–d* transitions while the second appears to be a phenolate–Cu(II) LMCT band.

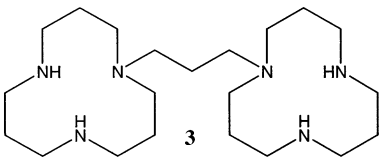

3

The bis-macrocyclic ligand **3**, incorporating two 12-membered tri-aza macrocycles linked via a propyl chain, forms a dinuclear Ni(II) complex of type $[Ni_2L(O_2CCH_3)_2(OH_2)_2](ClO_4)_2$ (L = **3**), the X-ray structure of which has been determined [23]. Each metal centre was shown to be bound to a *fac*-coordinated macrocyclic subunit and a bidentate acetate, with a water molecule completing the distorted octahedral coordination sphere. The metal centres are bound to the same 'inside' face of the ligand, with the macrocyclic rings adopting a face-to-face orientation. This arrangement facilitates formation of an intramolecular hydrogen bond (2.77 Å) between the water ligand of one Ni(II) ion and the acetate oxygen bound to the other. Magnetic measurements gave no evidence for coupling between metal centres.

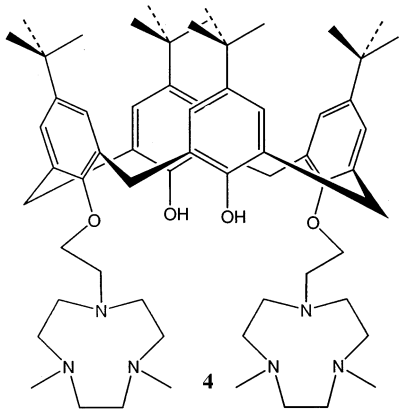

4

A substituted *p-tert*-butylcalix[4]arene moiety has been used as a framework for linking two *N*,*N*′-dimethyl(tacn) macrocycles through *N*-ethyl linkages to the 1,3-phenolic oxygens of the calix[4]arene to yield **4** [24]. Reaction of **4** with Ni(II) perchlorate in the presence of excess NaN_3 yielded $[Ni_2L(N_3)_3]ClO_4$ (L = **4**). An analogous synthetic procedure employing Ni(II) acetate resulted in isolation of the corresponding complex of type $[Ni_2(L-H)(N_3)_3]$. The X-ray structure of this latter product confirms its dinuclear nature. Each Ni(II) centre coordinated to a tacn moiety, with a distorted octahedral environment being achieved by end-on coordination of three 1,1-bridging azide ligands. The calix[4]arene framework adopts the familiar cone shape, encapsulating an acetonitrile molecule, with one of the phenol groups deprotonated. Magnetic susceptibility measurements indicate that the metal centres are ferromagnetically coupled, facilitated by the presence of the end-on bridging azide ligands; the Ni···Ni separation is 2.85 Å.

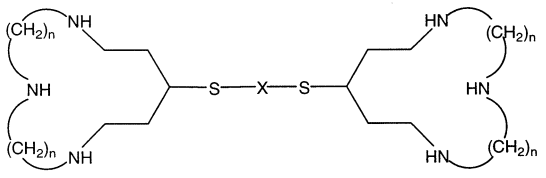

5a X = 1,3-phenyl; n = 2
5b X = 1,4-phenyl; n=2
5c X = 1,4-phenyl; n = 3
5d X = 4,4′-biphenyl; n = 2
5e X = $(CH_2)_5$; n = 2

Di-Zn(II) complexes of ligands of type **5** have been examined as catalysts for the hydrolysis of substrates that include *p*-nitrophenyl phosphate and the RNA dinucleotide 3′,5′-uridyluridine (UpU) [25]. The distance between the binding sites was observed to influence selectivity. Those systems incorporating a short phenyl spacer (**5a** and **5b**) were observed to promote hydrolysis of *p*-nitrophenyl phosphate since simultaneous binding of the phosphate group by the two Zn(II) ions is possible, a situation which is precluded for **5d** which incorporates a longer biphenyl spacer. When a flexible pentamethylene spacer was employed, as in **5e**, the di-Zn(II)

complex was shown to be a poor catalyst, thus indicating the importance of rigidity in these systems. The hydrolysis of UpU was most efficiently catalysed when the ligand **5d**, incorporating the biphenyl spacer, was employed. The proposed mechanism in this case involves intramolecular attack of the phosphodiester group coordinated to one Zn(II) by the 2′-alkoxide of the uridine moiety coordinated to the other Zn(II) ion.

2.2. Bis-macrocyclic ligands with pendant donors

The bis(tacn) motif incorporating aliphatic linkers has been modified by the attachment of acetate pendant-arms to the secondary nitrogens of each ring to give derivatives of type **6** [X = $(CH_2)_2$ or $(CH_2)_4$] [26]. In both cases the corresponding dinuclear Cu(II) complex of type $[Cu_2L]$ adopts an *anti* configuration in the solid state; the pseudo-square pyramidal coordination around each metal centre is composed of two monodentate carboxylate groups and the two nitrogen donors with pendant-groups forming the base, and the third nitrogen donor in the axial position.

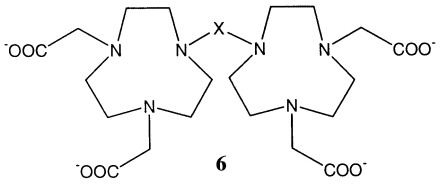

6

The complexation of Mn(II) by the analogous pyridylmethyl pendant derivatives **7** [X = $(CH_2)_2$, $(CH_2)_3$, $(CH_2)_4$, *m*-xylyl or $CH_2CH(OH)CH_2$] has also been investigated [27]. X-ray structures of the complexes of type $[Mn_2LCl_2](ClO_4)_4$, where L = **7** [X = $(CH_2)_2$, $(CH_2)_3$ or $(CH_2)_4$], have all been reported. In each case the coordination geometry of the metal centres is intermediate between trigonal prismatic and octahedral, with individual donor sets being made up of five nitrogen donors and a chloride ion adjacent to the nitrogen donor through which the two macrocycles are linked.

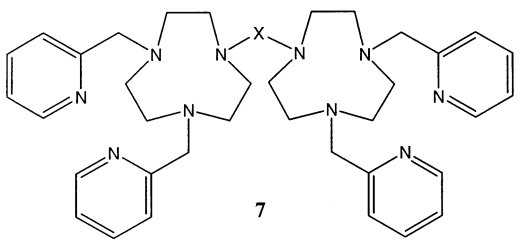

7

The room-temperature magnetic moments of the above complexes are all typical of high-spin Mn(II) species; variable-temperature magnetic susceptibility measurements and EPR spectra showed no evidence of coupling between metal centres.

Two waves corresponding to the di-Mn(II)/di-Mn(III) and di-Mn(III)/di-Mn(IV) oxidation events are present in the voltammograms of these simple alkyl-linked complexes, with the evidence suggesting that each wave reflects unresolved one-electron oxidation processes. The second oxidation wave is irreversible, presumably due to the decomposition of the unstable di-Mn(IV) species produced. As the alkyl chain is lengthened from ethyl to propyl to butyl, the $E_{1/2}$ potential of the first oxidation decreases ($E_{1/2} = +0.54$, $+0.52$ and $+0.49$ V vs. Fc/Fc^+, respectively), as does the $E_{1/2}$ for the second ($E_{1/2} = +1.34$, $+1.26$ and $+1.24$ V vs. Fc/Fc^+, respectively). These results support the idea that as the metal centres exert greater electrostatic influence on each other, oxidation becomes more difficult.

When the ligand contains a 2-hydroxypropyl linker, namely **7** [X = $CH_2CH(OH)CH_2$], three oxidation waves are present in the voltammogram. The first is attributed to two unresolved one-electron oxidations ($E_{1/2} = +0.52$ V vs. Fc/Fc^+) transforming the di-Mn(II) complex to di-Mn(III) as before. However, the second wave has been assigned to the one-electron oxidation ($E_{1/2} = +0.89$ V vs. Fc/Fc^+) of the di-Mn(III) complex to the mixed-valent Mn(III)–Mn(IV) state, the third wave being proposed to be a further one-electron oxidation ($E_{1/2} = +1.33$ V vs. Fc/Fc^+) to give the di-Mn(IV) species (which subsequently decomposes).

The dinuclear Mn(II) complexes of **7** [X = $(CH_2)_2$, $(CH_2)_3$, $(CH_2)_4$, *m*-xylyl or $CH_2CH(OH)CH_2$] were found to catalyse the disproportionation of H_2O_2 [27]; addition of H_2O_2 to DMF solutions of the above complexes resulted in vigorous evolution of dioxygen. However, dissociation of the complex also occurs during the catalytic cycling process, as evidenced by the precipitation of MnO_2 and the appearance of a signal in the EPR spectrum corresponding to $[Mn(OH_2)_6]^{2+}$. In the

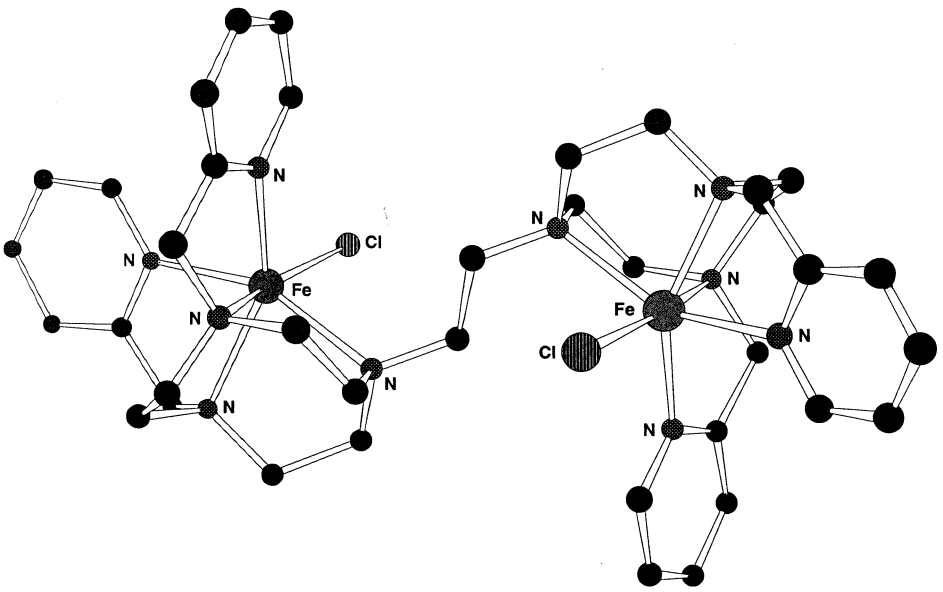

Fig. 5. The X-ray structure of the cation $[Fe_2LCl_2]^{2+}$ {L = **7** [X = $(CH_2)_2$]} [28].

case of the complex of **7** [X = $(CH_2)_2$], an intermediate mixed-valent species, attributed to a oxo-bridged Mn(III)–Mn(IV) species was observed in the EPR spectrum.

The structure of $[Fe_2LCl_2](PF_6)_2$, where L = **7** [X = $(CH_2)_2$] (Fig. 5), displays an *anti* configuration in which each metal is coordinated to a separate N_5-donor set from one half of the ligand [28]. A chloride ion completes the distorted octahedral coordination of each metal. The bright yellow product contains Fe(II) in its high spin state.

The di-Ni(II) complex $[Ni_2L(OH_2)_2](ClO_4)_4$, where L = **7** [X = $(CH_2)_4$], also adopts an *anti* configuration in the solid state [29]. The distorted octahedral geometry of each of the Ni(II) centres is defined by five nitrogen donors from one half of the linked ligand and a water molecule.

Communication was observed between the nickel centres in $[Ni_2L(OH_2)](ClO_4)_2$ where L = **7** [X = $(CH_2)_2$] using voltammetry. The presence of two partially resolved oxidation waves ($E_{1/2}$ = +1.11 and +1.17 V vs. Fc/Fc^+) separated by 60 mV, indicate that once the first Ni(II) centre has been oxidised, the oxidation of the second nickel centre becomes more difficult, as expected from the higher positive charge now present. However, corresponding communication between metal centres is not observed for the complexes of the propyl-, butyl- or *m*-xylyl-linked ligands. In the case of **7** [X = $CH_2CH(OH)CH_2$], where the linker contains a potential coordinating group, two partially resolved oxidation waves are again observed ($E_{1/2}$ = +1.06 and +1.17 V vs Fc/Fc^+). It is proposed that the alcohol group coordinates to the Ni(III) centre created after the first oxidation, bringing the two metal centres closer together, thus inhibiting the second oxidation step.

Dinuclear Cu(II) complexes of type $[Cu_2L](ClO_4)_4$, where L = **7** [X = $(CH_2)_2$ or $(CH_2)_4$], display similar *anti* configurations in the solid state to those mentioned above [30]. When the linker is a propyl unit as in **7** [X = $(CH_2)_3$], the X-ray structure of the corresponding dinuclear Cu(II) complex, $[Cu_2L](ClO_4)_4$, shows that it adopts a *syn* conformation. EPR demonstrated an inverse relationship between linker chain length and dipole-dipole coupling between the respective metal centres in this series of complexes. The weak interaction observed in the spectrum of the ethyl-bridged ligand complex is even less pronounced for the propyl-linked system, while the spectra of the butyl- and corresponding *m*-xylyl-linked ligand complexes closely matched that of the analogous monomeric bis(pyridylmethyl) pendant-arm derivative complex. Voltammetic analysis of all of the above di-Cu(II) complexes revealed that each undergoes a closely-spaced unresolved two electron reduction process – as expected for near non-interacting Cu(II) centres.

Zn(II) complexes of pyridylmethyl pendant ligands of the above type have also been investigated [31]. The X-ray structure of the dinuclear Zn(II) complex $[Zn_2LBr_2](ClO_4)_2$, where L = **7** [X = $(CH_2)_2$], shows a distorted octahedral geometry around each metal centre, made up of five nitrogen donors from one half of the ligand and a bromide ion. The complex adopts an *anti* configuration in the solid state with the metal–metal separation being 6.55 Å. The inclusion of a 2-hydroxypropyl linker as in **7** [X = $CH_2CH(OH)CH_2$], once again brings the metal centres into much closer proximity (3.90 Å); the X-ray structure of the Zn(II) complex is

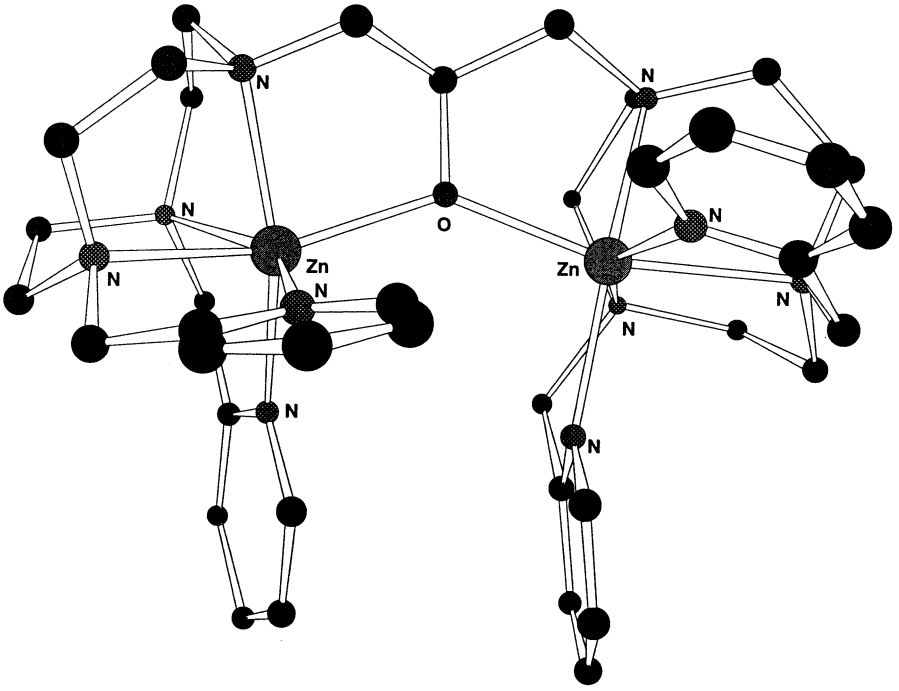

Fig. 6. The X-ray structure of the cation $[Zn_2L]^{3+}$ {L = **7** [X = $CH_2CH(O^-)CH_2$]} [31].

shown in Fig. 6. On complexation, the hydroxy group deprotonates and the resulting alkoxide ion bridges the metal centres.

2.3. Tris- and poly-macrocyclic ligands

The tris(tacn) macrocylic ligand **8** has been reported [32]. It yields a trinuclear Cu(II) complex formulated as $[Cu_3L(H_2O)_6](ClO_4)_6.6H_2O$ (L = **8**), that shows no evidence for magnetic interaction between the metal centres. Reaction of this

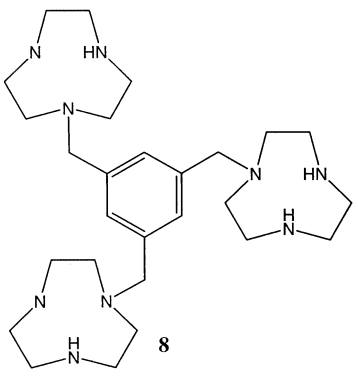

8

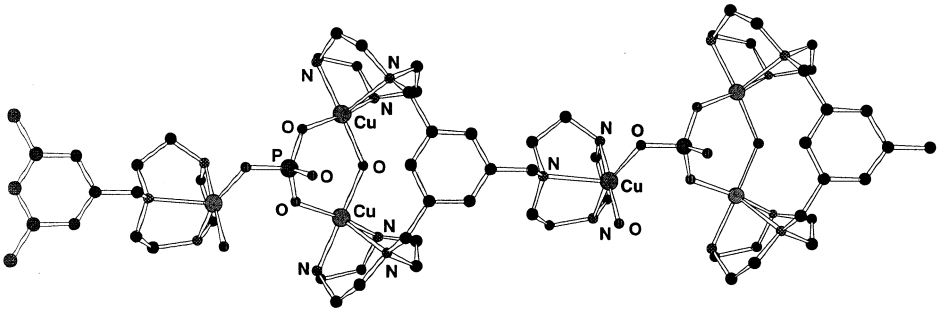

Fig. 7. The X-ray structure of the repeating cation unit $[Cu_3L(\mu\text{-}OH)(\mu_3\text{-}HPO_4)(OH_2)]^{3+}$ (L = **8**) [32] in $\{[Cu_3L(\mu\text{-}OH)(\mu_3\text{-}HPO_4)(OH_2)](PF_6)_3.3H_2O\}_n$.

complex with a source of phosphate in the presence of PF_6^- results in the isolation of a polymeric species of type $\{[Cu_3L(\mu\text{-}OH)(\mu_3\text{-}HPO_4)(OH_2)](PF_6)_3\cdot 3H_2O\}_n$ (L = **8**) (Fig. 7). The X-ray structure shows that the $[LCu_2(\mu\text{-}OH)(\mu_3\text{-}HPO_4)Cu(OH_2)]^{3+}$ cationic unit incorporates three Cu(II) ions coordinated to the individual tacn rings of **8**. Each metal resides in a tetragonally distorted square pyramidal coordination environment, the basal plane of which is defined by the secondary nitrogens of a tacn ring and two oxygen donors, with the tertiary amine occupying the apical position. The oxygen donors for two of these metal centres are provided by a bridging hydroxide ion as well as an oxygen to each from the μ_3-phosphate anion; the copper–copper distance between these two centres being 3.56 Å. The phosphate also coordinates to a third Cu(II) belonging to a neighbouring ligand, resulting in the polymeric structure; the coordination geometry of this latter copper ion is completed by a water molecule. The inter-ligand metal–metal distances between this centre and the two Cu(II) ions with which it shares a phosphate bridge are much shorter (4.56 and 5.47 Å) than those to the two Cu(II) ions which are coordinated to the same ligand (9.28 and 9.43 Å). While the latter distances preclude the likelihood of a magnetic interaction involving these ions, fitting of the magnetic susceptibility data for the complex suggested that anti-ferromagnetic coupling occurs between the Cu(μ-OH)(μ-HPO_4)Cu bridged centres as well as between these centres and the third phosphate bridged centre.

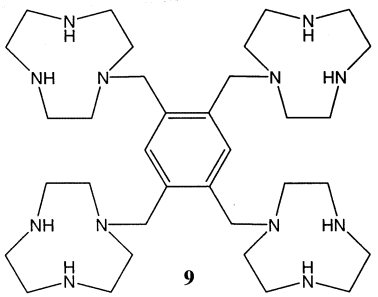

9

Several modes of metal coordination have been observed for the tetramacrocyclic system **9**: di-, tri- and tetranuclear species have all been observed to form [33].

Reaction of **9** with four equivalents of Ni(II) resulted in a mixture of di- and trinuclear complexes, $[Ni_2L](ClO_4)_4$ and $[Ni_3L(OH_2)_6](ClO_4)_6$ (L = **9**), which are readily separated by cation exchange chromatography. The tetranuclear complex, $[Ni_4L(OH_2)_{12}](ClO_4)_8$ (L = **9**), was also obtained as an equimolar mixture with the trinuclear complex when **9** was added to a large excess (50 equivalents) of nickel ion. In contrast, the di- and tetra-Cu(II) complexes were obtained on reaction of **9** with two and four equivalents of copper ion, respectively.

An X-ray study of $[Ni_2L](ClO_4)_4$ (L = **9**), reveals that the two pairs of *ortho*-related tacn macrocycles sandwich each Ni(II) ion to complete a distorted octahedral coordination geometry for each. The two metal centres are situated on opposite sides of the plane of the aromatic linker at a distance of 9.09 Å. The distortion from octahedral geometry arises from steric constraints imposed by the ligand and the lengthening of the tertiary N–Ni bond (2.19 Å), coupled with a shortening of the corresponding *trans* bonds (2.09–2.15 Å). A similar structure is present in the di-Cu(II) analogue, with the intramolecular metal–metal separation being 8.90 Å; however, in the latter case the coordination geometry of each Cu(II) (d^9) also shows the presence of a Jahn–Teller distortion.

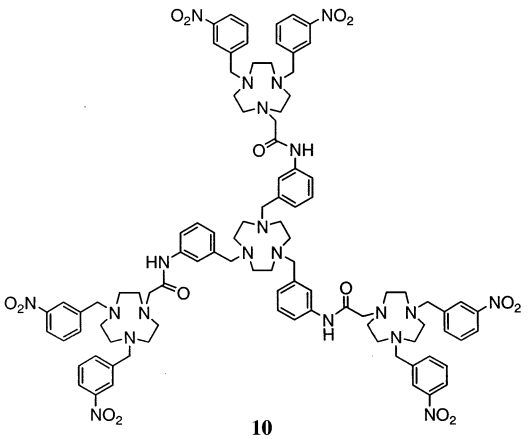

10

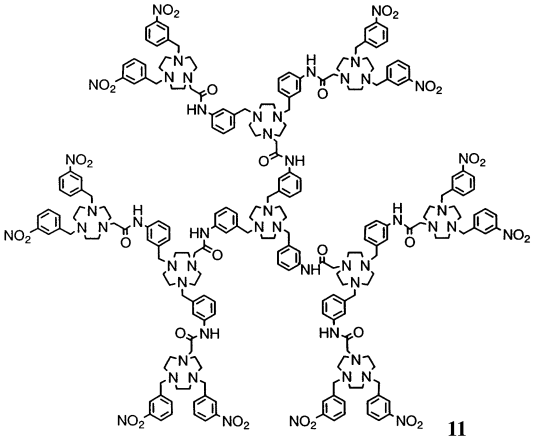

11

The sandwich configuration of one pair of *ortho*-related tacn rings is again observed in the crystal structure of the trinuclear Ni(II) complex $[Ni_3L(OH_6)](ClO_4)_6$ (L = **9**), with the remaining two rings binding one metal centre each with water molecules completing their distorted octahedral geometries. The two NiN_3O_3 centres lie on opposite sides of the plane of the aromatic linker, with the nickel ions separated by 6.97 Å.

In $[Cu_4L(OH_2)_8](ClO_4)_8$ (L = **9**), each metal is coordinated to a separate tacn subunit as well as to two water molecules. The secondary amines and the waters around each copper form the basal plane of a square pyramid while the axial position is occupied by the tertiary amine. The arrangement of the ligand is such that *ortho*- and *para*-related macrocyclic compartments are *anti*, the shortest metal–metal distance being 7.04 Å between *ortho*-related pairs. Magnetic susceptibility measurements and EPR spectra confirmed the absence of coupling between metal centres in this complex.

Incorporation of tacn into dendritic architectures has also been reported, with the tetra- and deca-macrocyclic species **10** and **11** having been synthesised [34]. Spectrophotometric titrations in acetonitrile and DMF indicate that, under the conditions employed, these ligands bind four and ten Cu(II) ions, respectively.

3. Linked tetra-aza and higher aza ring systems

3.1. Bis-macrocyclic ligands

The usual requirement for suitable *N*-protected macrocyclic derivatives for the synthesis of linked ring systems [2] has been circumvented in the case of a series of bis(tetraaza[14]paracyclophanes) of type **12** through use of the Zn(II) complex as a precursor for the linking reaction [35]. Only three of the four nitrogen donors of each parent (non-linked) ring are capable of coordinating to a single Zn(II) ion, due to steric constraints arising from the presence of the aromatic moiety in the ring. This effectively leaves one of the benzylic nitrogens of each ring free for further functionalisation. In this way, reaction of the Zn(II) complex with the appropriate bis(halomethyl)arene allowed isolation of the corresponding bismacrocyclic ligand

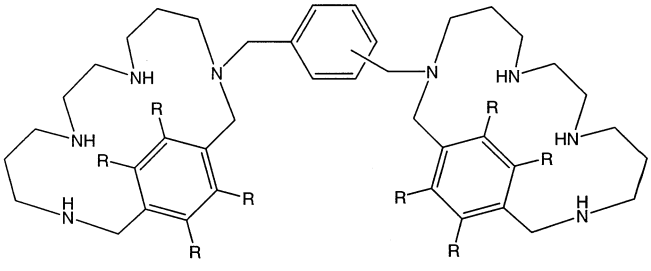

12a *para*-, R = H
12b *para*-, R = CH_3
12c *meta*-, R = H
12d *meta*-, R = CH_3

12

of type **12** in up to 87% yield. Potentiometric log K measurements for complexation of the octamethyl derivative **12d**, show that both mono- and dinuclear Cu(II) complexes are formed ($\log K_{CuL} = 13.46$ and $\log K_{Cu2L} = 8.8$).

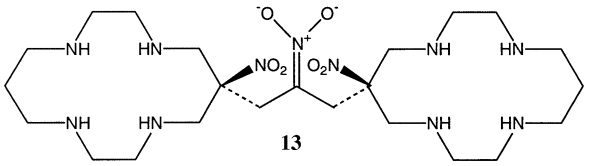

13

The di-Cu(II) complex of the nitronate bridged ligand **13** was isolated from a metal template reaction as a dimer [36]. The product, $[Cu_2LCl_3]_2(ClO_4)_3$ (L = **13**), has been studied in the solid state. The X-ray structure shows that one of the cyclam-bound Cu(II) metal centres binds to a nitronate oxygen of a neighbouring ligand ($Cu–O^- = 2.41$ Å) and vice versa for a second Cu(II). A distance of 11.32 Å separates the Cu(II) ions of the covalently-linked macrocycles. The tetragonally elongated octahedral coordination environments of the respective Cu(II) ions are completed by either chloride or perchlorate anions. The EPR spectrum of $[Cu_2LCl_3]_2(ClO_4)_3$ (L = **13**) as a frozen water–DMF solution is consistent with a weakly dipole–dipole coupled di-Cu(II) complex with a Cu···Cu separation of about 11 Å, indicating that the compound exists as a discrete monomer in solution and not as the dimer identified in the solid-state.

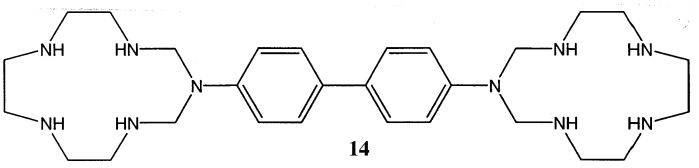

14

A range of dinuclear complexes of the biphenyl-linked ligand **14** have been synthesised. These are of types $[M_2LCl_4]$ and $[M_2L(NO_3)_4]$ (L = **14**), where M = Mn(II), Co(II), Ni(II), Cu(II) and Zn(II) [37]. Spectroscopic evidence suggests that the coordination environments of the metal centres are distorted octahedral, being composed of the macrocyclic secondary amines and chloride or monodentate nitrate groups — the latter coordinating in the axial positions. Magnetic moments and EPR spectra for the di-Cu(II) complexes give no evidence for metal–metal interaction, as expected from the use of an elongated rigid biphenyl spacer to separate the metal centres.

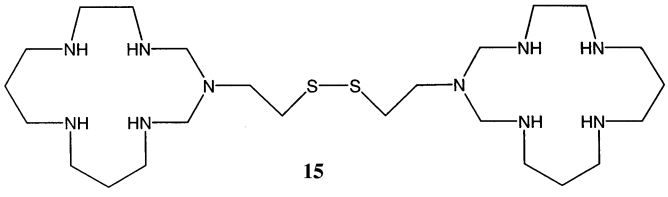

15

The Ni(II) and Cu(II) complexes of bis(pentaazamacrocyclic) ligand **15** were synthesized by the template condensation of bis(2-aminoethyl)-1,3-propanediamine, formaldehyde and 2-aminoethyl disulfide [38]. In solution, a thermodynamic equilibrium between yellow (low-spin) and blue (high-spin) species occurs for the di-Ni(II) complex of this ligand.

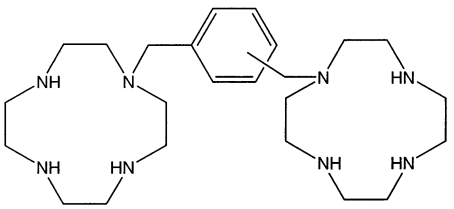

16a *para-*
16b *meta-*

The di-Zn(II) complex of the linked bis(cyclen) ligand **16a** (cyclen = 1,4,7,10-tetraazacyclododecane) has been investigated as a receptor for barbituates in aqueous solution [39]. Potentiometric titrations ($5 < pH < 10$) reveal that the di-Zn(II) complex $[Zn_2L(OH_2)_2](ClO_4)_4$ (L = **16a**) sequesters the dianion of barbital to form both 1:1 and 2:2 host-guest complexes. The crystal structure (Fig. 8) of the 2:2 complex, $[\{Zn_2L(barbital)\}_2]^{4+}$ (L = **16a**), shows that intermolecular bridging of two Zn_2L (L = **16a**) units occurs through $Zn-N^-$ bonds to the barbital dianions. Each Zn(II) is situated in a distorted tetragonal pyramidal coordination environment, with short $Zn-N^-$ bonds (1.95–1.99 Å) being evident in comparison to the Zn–N bonds of the macrocyclic donors (2.10–2.22 Å) [displaying the preference of the strongly acidic Zn(II) for anionic over neutral *N*-donors].

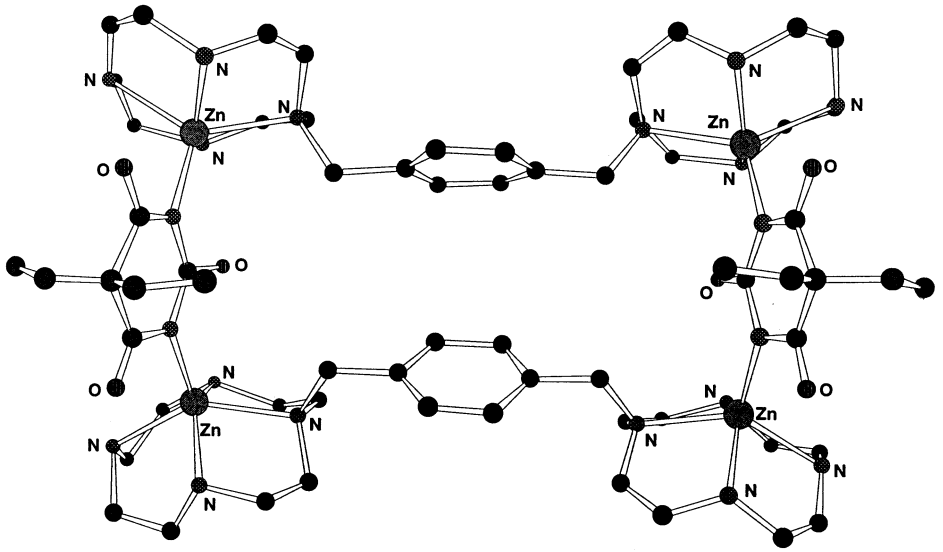

Fig. 8. The X-ray structure of the cation $[\{Zn_2L(barbital)\}_2]^{4+}$ (L = **16a**) [39].

The di-Zn(II) complex of the *m*-xylyl-linked bis(cyclen) ligand **16b** also binds barbital, forming a stable 1:1 complex in aqueous solution [40]. This ligand also has a strong affinity for the (bidentate) phosphomonoester dianion, 4-nitrophenyl phosphate. The isolation of $[Zn_2L(OH)(OH_2)](ClO_4)_3$ (L = **16b**) supports the solution behaviour postulated from the pH/NMR titration data, that intramolecular hydrogen-bonding between a hydroxide ion and water ligands bound to the Zn(II) metal centres occurs in solution [41].

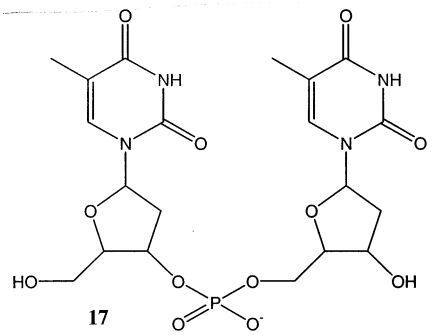

17

$[Zn_2L(OH_2)_2](ClO_4)_4$ (L = **16a**) has also been investigated as a receptor for thymidylythymidine (TpT) **17** (as a model for DNA and RNA binding) [42]. Indeed, NMR studies indicated that the complex was capable of binding TpT via two $Zn-N^-$ bonds involving deprotonated imides that coordinate to separate metal centres. Extension of these studies has revealed that the di-Zn(II) complexes of both **16a** and **16b** act as highly selective and efficient hosts for thymidine nucleotides (such as thymidine 5′-monophosphate) at physiological pH in aqueous solution [43]. It is postulated that the stability of the 1:1 adducts formed reflects the additive binding effect of the deprotonated thymine imide functionality and the terminal phosphate dianion interacting with separate Zn(II) centres of the dinuclear complex. Furthermore, the *p*-isomer was generally a better receptor than the *m*-isomer, most likely due its dimensions being more suitable for promoting enhanced interaction.

3.2. Tris-macrocyclic ligands

Paralleling the binding between $[Zn_2L(OH_2)_2](ClO_4)_4$ (L = **16a**) and thymidylythymidine (TpT) **17**, described above, an adduct is also formed between the tri-Zn(II) complex of the linear tris(cyclen) ligand **18** and the corresponding trifunctional species thymidylthymidylythymidine (TpTpT) **19** [42].

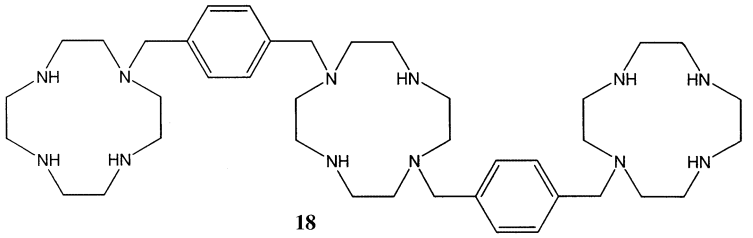

18

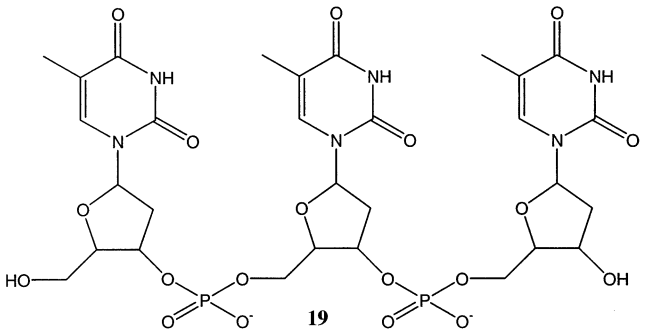

19

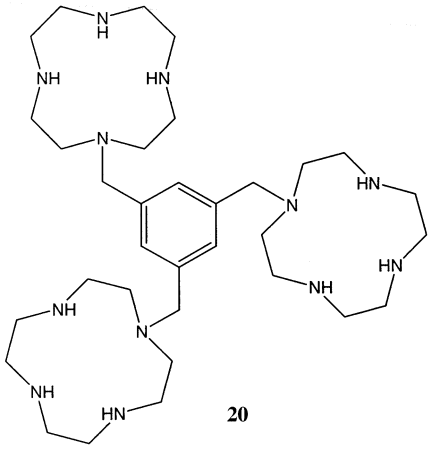

20

A potentiometric (pH) titration of the tri-Zn(II) complex of tris(cyclen) ligand **20** coupled with an investigation of NMR spectral changes against p*D* suggested that a hydrogen-bonding arrangement between bound water and hydroxide ligands occurs for this species at neutral pH in a similar way to that observed for the di-Zn(II) complex of **16b** in aqueous solution [41]. Intramolecular bridging between the metal centres was also postulated, possibly involving a tridentate phenylphosphate dianion. An X-ray structure of $[Zn_3L(NO_3)_2(OH_2)](NO_3)_4$ (L = **20**), reveals that each metal centre is bound to one macrocyclic ring. The metal ions reside on an equivalent face of each ring such that a distorted tetragonal-pyramidal coordination sphere is formed, an apical *O*-donor being provided by a nitrate ion for two of the metal centres, while this position in the third is occupied by a water molecule. The trinuclear zinc complex was shown to be a much better host towards organic phosphate dianions in aqueous solution than is the parent $Zn(cyclen)^{2+}$ complex.

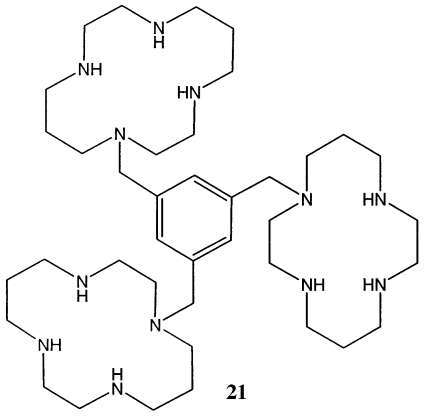

21

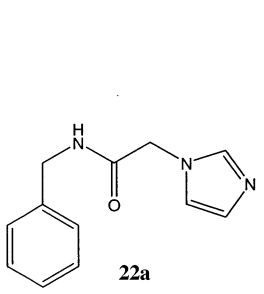

22a

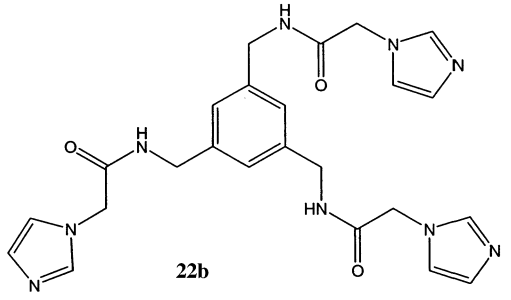

22b

The binding of histidine guests to the tri-Hg(II) complex of the tris(cyclam) ligand **21** (cyclam = 1,4,8,11-tetraazacyclotetradecane), has been investigated [44]. A NMR titration confirmed that $[Hg_3L](ClO_4)_6$ (L = **21**), binds three equilavents of the imidazole-containing molecule **22a**. When the three imidazole moieties are linked into the one ligand as in **22b**, a 1:1 complex is observed.

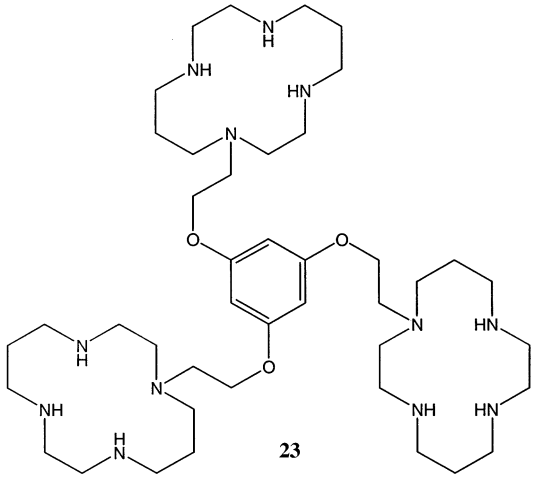

23

The synthesis of the tri-linked species **23**, incorporating a phloroglucinol core has been achieved [45]. An initial study has involved the interaction of **23** with Ni(II) and Cu(II). Both form 3:1 (metal:ligand) species; these have been isolated and characterised.

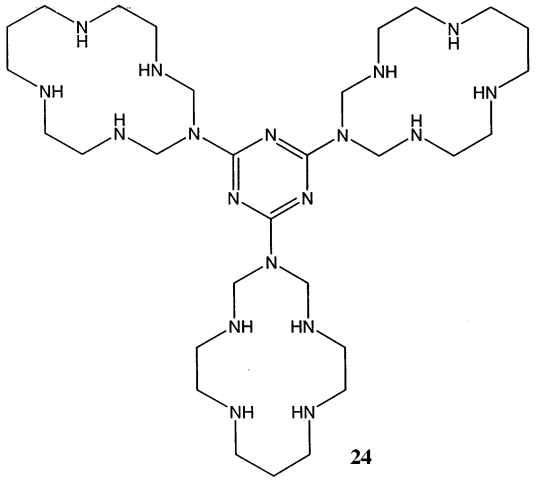

24

A Cu(II)-directed condensation reaction has been used to synthesise **24** and the structure of the resulting tri-Cu(II) complex $[Cu_3L](ClO_4)_6$ (L = **24**) was determined by X-ray diffraction [46]. Each Cu(II) ion is bound by four secondary amines from a macrocyclic subunit, with *O*-donors occupying the axial positions from either a water or a perchlorate anion (at distances of ca. 2.5 Å). One of the macrocyclic subunits resides on the opposite side of the plane of the aromatic core to the other two, the metal–metal distances between the *syn* Cu(II) centres being shorter (7.97 Å) than that between *anti* metal ions (9.36 and 9.54 Å). Despite these internuclear distances, weak three-way dipole-dipole coupling interactions were detected in the corresponding EPR spectrum. The square wave voltammogram displays a one-electron and a two electron reduction wave at -1.14 and -1.35 V (vs. Fc/Fc^+), respectively, and is hence in accordance with electrostatic interactions being present between the metal centres.

3.3. Tricyclic ligands

Potentiometric titration studies indicated that the tricyclic ligands **25** and **26** both form mono- and dinuclear complexes in solution [47]. The stability constants in aqueous media ($I = 0.1$, NEt_4ClO_4) for the complexes of **25** with Cu(II), Zn(II), Cd(II) and Pb(II) are: (log K_{ML}) 17.64, 10.84, 9.5 and 8.75, respectively, (log K_{M2L})

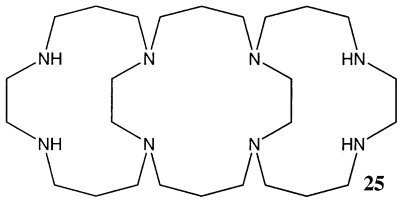

25

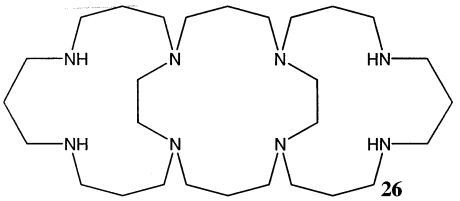

26

13.75, 6.65, 5.6 and 4.9, respectively. These values correspond to complexation of the first and second metal ions in the outer compartments of this tricyclic ligand — undoubtedly reflecting the stronger coordinating ability of the secondary amines as well as the need to minimise electrostatic interactions between the metal ions once they are bound. The isolation of di-halide (or pseudo-halide) species of type $[Cu_2LX_2](ClO_4)_2$ (L = **25**), where $X = Cl^-$, Br^-, I^- and SCN^-, suggested that terminal anion binding occurs. Indeed, these complexes appear to show little tendency for forming bridges between their metal centres. This postulate was supported by the absence of corresponding isosbestic points in the spectrophotometric titration of $[Cu_2L](ClO_4)_4$ (L = **25**) with several coordinating anions.

The crystal structure of $[Cu_2Cl_2L]Cl_2.2H_2O$ (L = **25**) shows that the Cu(II) ions are situated in the outer compartments of **25**, each in a distorted square-pyramidal coordination sphere with a coordinated chloride ion occupying the apical site. While the complex adopts an overall boat-like conformation, the chloride ions occupy terminal binding sites such that they are directed away from the other metal centre; the metal–metal separation is 5.2 Å.

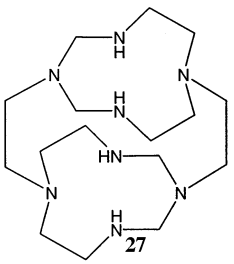

27

The linking of two 10-membered tetraaza macrocyclic units in a co-facial arrangement has been accomplished in a metal templated one-pot reaction [48]. An excess of formaldehyde was reacted with a 1:2 molar mixture of Ni(II) and tris(2-aminoethyl)amine (tren) to yield the mononuclear complex $[NiL](ClO_4)_2$ (L = **27**). The magnetic moment of this purple species (2.95 BM) at room temperature is typical of high-spin Ni(II). The complex is resistant to demetallation by boiling aqueous cyanide solution; however, slight decomposition is observed in 0.5 M HCl at room temperature. In strong acid (6 M HCl) at elevated temperatures, decomposition is rapid. However, efforts to isolate the free ligand were unsuccessful, with $[Ni(tren)_2](ClO_4)_2$ being the only product obtained. The crystal structure of the Ni(II) complex of **27** shows that the ligand coordinates in a hexadentate fashion such that it encapsulates the Ni(II) ion to yield a tetragonally distorted coordination geometry. In this arrangement, both tertiary nitrogens associated with the $N–CH_2–N$ chains remain uncoordinated.

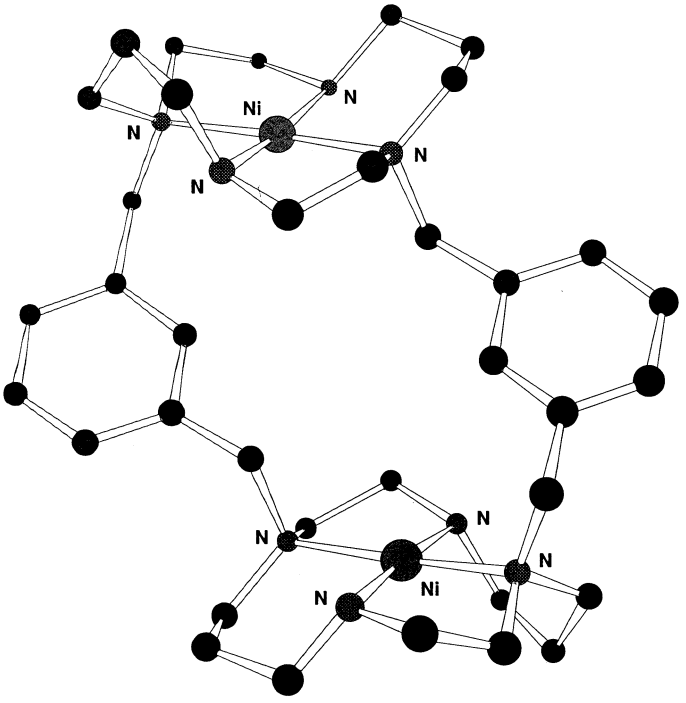

Fig. 9. The X-ray structure of the cation $[Ni_2L]^{2+}$ (L = **28a**) [52].

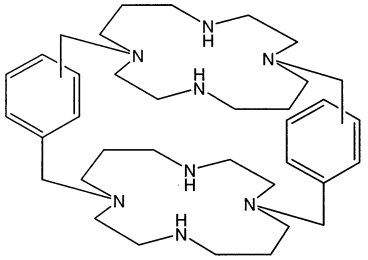

28a *meta-, meta-*
28b *para-, para-*

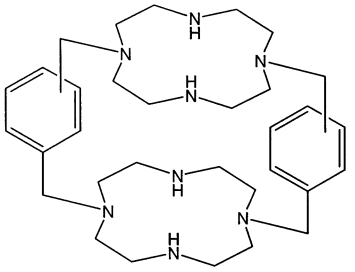

29a *meta-, meta-*
29b *para-, para-*
29c *meta-, para-*

Guilard and co-workers have devised synthetic methodology for obtaining co-facial bis(tetraaza) macrocyclic ligands of type **28** and **29** [49–52]. Macrocyclic ligands **28a** and **28b** were isolated and characterised as their di-Cu(II) and di-Ni(II) complexes, $[Cu_2L](ClO_4)_4$ and $[Ni_2L](ClO_4)_4$ (L = **28a** or **28b**) [52]. The UV–vis spectra of $[Cu_2L](ClO_4)_4$ (L = **28a** or **28b**) in acetonitrile display a broad absorption due to d–d* transitions with a λ_{max} of 520 nm, in accordance with the presence of a CuN_4 chromophore, and a LMCT band at λ_{max} ca. 345–350 nm. IR spectra showed no evidence for the presence coordinating perchlorate anion. The EPR spectra of $[Cu_2L](CH_3COO)_4$ (L = **28a** or **28b**) are indicative of triplet states resulting from an exchange-coupled pair of Cu(II) ions. From these studies metal–metal distances of 6.5 and 7.4 Å (respectively) were estimated. The electronic, infrared and EPR spectra were all consistent with the presence of a square planar Cu(II) coordination geometry in these complexes.

The UV–vis spectra of the yellow di-Ni(II) complexes of type $[Ni_2L](ClO_4)_4$ (L = **28a** or **28b**) in acetonitrile each show a broad absorption with λ_{max} at ca. 480 nm ($\varepsilon = 260–270\ M^{-1}\ cm^{-1}$). This is characteristic of the presence of diamagnetic square planar Ni(II), with no evidence for an equillibrium between high- and low-spin states being present under the conditions employed. Once again, the infrared spectrum gave no evidence for perchlorate coordination.

The X-ray structure of $[Ni_2L](ClO_4)_4{\cdot}2CH_3CN$ (L = **28a**) (Fig. 9) has been determined and is in accord with the above observations. Each Ni(II) is bound in a square planar arrangement to the four nitrogen donors of a separate cyclam subunit. The *N*-substituents of the cyclam units all lie on the same side of the respective macrocyclic planes (*trans* I). The metal centres are separated by 6.83 Å, comparable to the intermetallic distance (estimated) in the analogous di-Cu(II) complex of 6.5 Å.

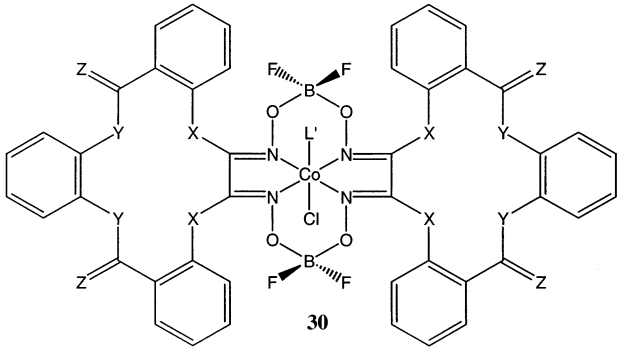

30

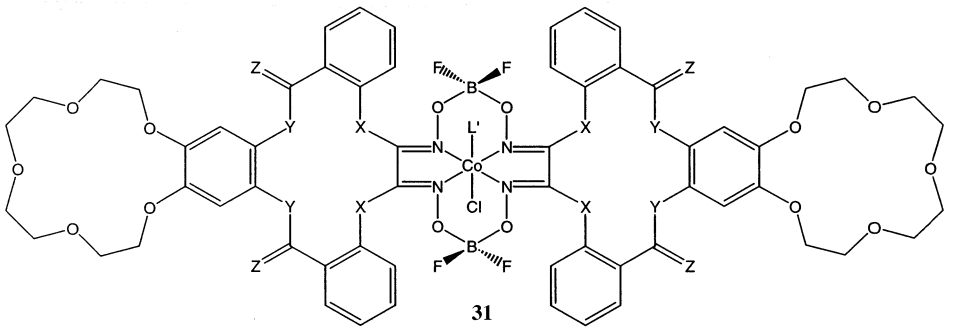

31

Coordination of vicinal dioximes has been employed to obtain the linked macrocyclic ligand complexes of types **30** (X,Y = NH; Z = H,H; L′ = pyridine) and **31** (X,Y = NH; Z = H,H; L′ = pyridine) [53,54]. The template synthesis of these products involves the linking of two tetraazamacrocycle-containing components through dioxime coordination to Co(II), then aerial oxidation of this ion to Co(III) in the presence of (axial coordinating) pyridine and chloride ligands. The intermolecular hydrogen bonds between the coordinated oximes are then replaced by BF_2^+ groups by reaction with boron trifluoride etherate to yield the linked bis-macrocyclic ligand complex **30** (X,Y = NH; Z = H,H; L′ = pyridine) or **31** (X,Y = NH; Z = H,H; L′ = pyridine); the reaction involving BF_3 is a long established procedure [55]. Trinuclear complexes of type $[Cd_2CoL]Cl_2$ where CoL = **30** (X,Y = NH; Z = H,H; L′ = pyridine), and $[Cu_2CoL](PF_6)_2$ where CoL = **31** (X,Y = NH; Z = H,H; L′ = pyridine), are readily formed on addition of $CdCl_2$ or $[Cu(CH_3CN)_4]PF_6$ to the respective Co(III)-containing species.

4. Linked mixed-donor ring systems

Ligands with mixed N_2S_2-donor sets have been used for the synthesis of trinuclear complexes of type $[Pd_2CoL]$ where CoL = **30** (X = S; Y = N; Z = O; L′ = 2,6-lutidine), **31** (X = S; Y = N; Z = O; L′ = pyrimidine), **32** (X = S; Y = N; L′ = pyrimidine) or **32** (X = N; Y = S; L′ = pyrimidine) [56,57]. Furthermore, the

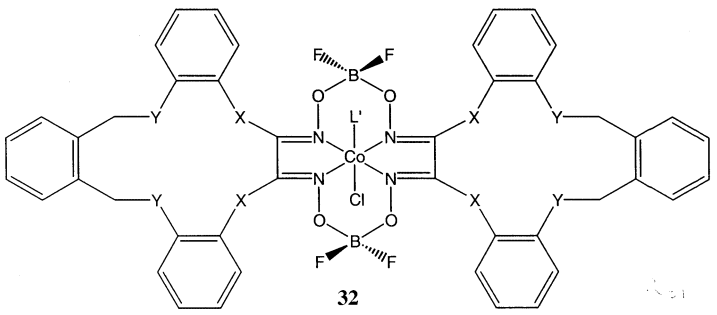

32

N_2S_2-donor spiro-linked macrocycle **33** has been linked via its dioxime groups to give the polymeric complex **34** (X = NH; L′ = pyrimidine) [58]. Reaction of **34** (X = NH; L′ = pyrimidine) with bis(benzonitrile)palladium(II) chloride yields the heteropolynuclear complex $[Pd_2CoL]_n$ where CoL = **34** (X = N; L′ = pyrimidine). A further example of a heteropolynuclear complex was obtained on reaction of **35** (X = NH; L′ = pyridine) with copper(II) acetate to give the complex $[Cu_2CoL]_n$ where CoL = **35** (X = N; L′ = pyridine) [59].

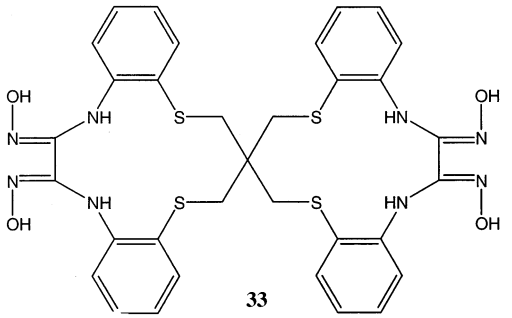

33

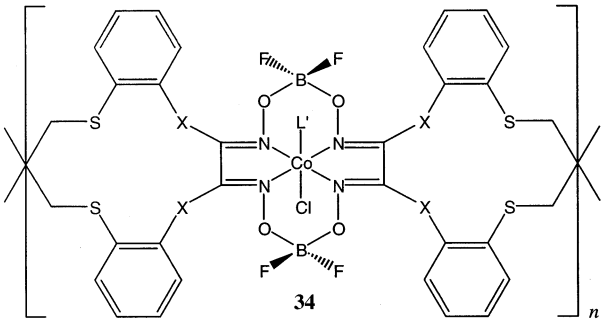

34

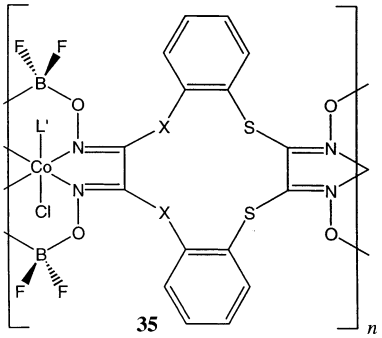

35

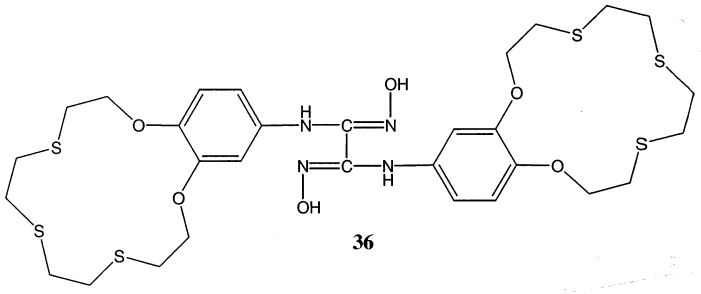

36

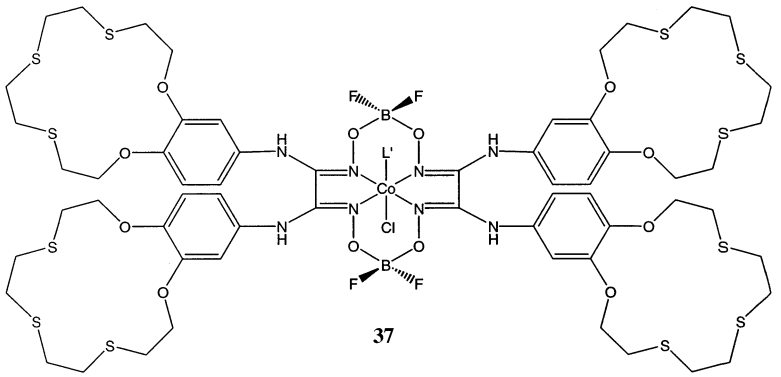

37

The O_2S_3-donor ligands **36** and **37** (L′ = pyridine) have been employed as the ionophore (1×10^{-4} mol dm^{-3}) in the organic phase in solvent extraction experiments (water–chloroform) in which the aqueous phase contained Ag(I) or Hg(II) nitrate (2×10^{-5} mol dm^{-3}) and picric acid (2×10^{-4} mol dm^{-3}) [60]. The bis(macrocyclic) ligand **36** was found to extract 79% of the Ag(I) present while the extraction of Hg(II) was negligible. In part, this selectivity may reflect the poor fit of Hg(II) for the O_2S_3 macrocyclic cavity. However, in separate experiments, high extraction of both Ag(I) (92%) and Hg(II) (94%) was achieved using **37** (L′ = pyridine).

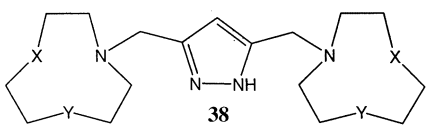

38

Kaden and co-workers have synthesised bis(macrocyclic) ligands of type **38** incorporating N_3-, N_2S- and NS_2-donor cyclononane units linked by a pyrazole-containing group [61–64]. In $[Ni_2L(N_3)(OH_2)_2](ClO_4)_2$, where L = **38** (X, Y = NH), the metal centres are bridged through separate ends of the 1,3-azide ligand; the intermetalic separation being 4.45 Å [61]. A distorted octahedral geometry is observed for each Ni(II), with each being bound to three *N*-donors of a macrocyclic subunit, a pyrazolide, an azide N^- donor and a water molecule. The relative arrangement of the two macrocyclic subunits is *transoid*.

The di-Cu(II) complexes of type $[Cu_2LX]^{n+}$ (L = **38**) where $X = Cl^-$, Br^-, SO_4^{2-} or N_3^- have been reported [62]. In these, each metal is bound to a tridentate macrocyclic subunit as well as to a deprotonated pyrazole group and a bridging anionic ligand. The coordination geometry of the Cu(II) ions in $[Cu_2L(N_3)](PF_6)_2$, where L = **38** (X, Y = NH), is a distorted square pyramid, the Cu···Cu separation being 4.15 Å. Each metal centre is bridged through separate ends of the azide ligand. The base of the square pyramidal geometry is defined by a deprotonated pyrazole group, the azide ligand and a secondary and tertiary amine from a macrocyclic subunit; there is also a bond to the remaining secondary amine. The latter occupies the axial position with the Cu–N length (2.16–2.18 Å) being distinctly longer than the Cu–N bonds (1.93–2.07 Å) in the base. Both metal centres, the pyrazole *N*-atoms, and the azide ion form a nearly planar arrangement.

Both $[Cu_2LCl](ClO_4)_2$ and $[Cu_2LBr](ClO_4)_2$, where L = **38** (X, Y = S), contain similar distorted trigonal pyramidal coordination geometries around each Cu(II) ion, with the metal–metal distances in both complexes also being similar (3.70 and 3.76 Å, respectively). The axial positions of the distorted trigonal pyramid are occupied by a bridging halide ion and a tertiary nitrogen.

Interestingly, the X-ray structure of $[Cu_2L(SO_4)](PF_6)$ where L = **38** (X = NH; Y = S) (Fig. 10), shows that each Cu(II) ion is in a different environment. One Cu(II) centre has a distorted trigonal bipyramidal coordination geometry, with the macrocyclic N and sulfato O occupying the axial positions. However, the second Cu(II) has a distorted octahedral geometry with a water taking up the sixth position. The separation of the Cu(II) ions is 4.16 Å.

In the case of the di-Cu(II) complexes of the above ligand systems, anti-ferromagnetic coupling between the metal centres is observed, especially when a bridging azide ligand is present. For $[Cu_2L(N_3)](PF_6)_2$, where L = **38** (X, Y = NH), the magnetic moment at room temperature is 1.30 BM (compared to an expected value of ca. 3.4 BM for two non-interacting Cu(II) ions) and is comparable to the value obtained in aqueous solution (1.36 BM), strongly suggesting that the dinuclear structure found in the solid state remains essentially intact in solution [61]. The room temperature magnetic moment for $[Cu_2L(N_3)]^{2+}$, where L = **38** (X = NH; Y = S), is also 'low' at 0.94 BM [62]. The low magnetic suscepibility χ_{mol} over a wide temperature range ($-2J > 1000$ cm^{-1}) of both azide bridged complexes indicates the presence of an especially strong anti-ferromagnetic couple. In contrast, $[Cu_2L(1H\text{-pyrazol-1-ide})]^{2+}$, where L = **38** (X = NH; Y = S), and $[Cu_2LCl]^{2+}$, where L = **38** (X, Y = S), exhibit anti-ferromagnetic coupling ($-2J = 300$ and 272 cm^{-1}, respectively) only at low temperature; whereas at room temperature their respective magnetic moments are 2.84 and 2.74 BM.

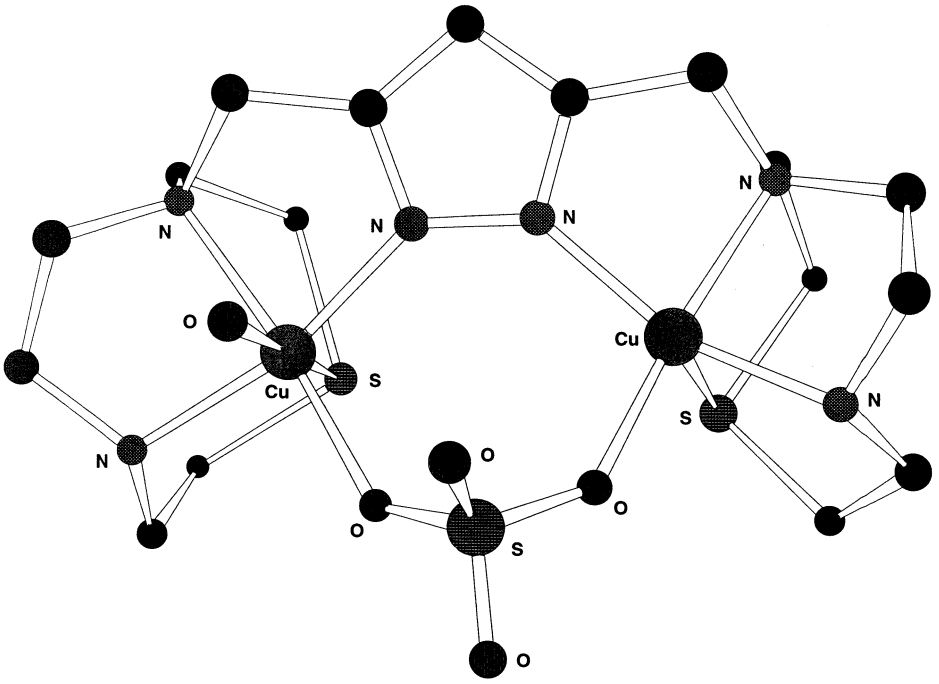

Fig. 10. The X-ray structure of the cation $[CuL(SO_4)]^+$ [L = **38** (X = NH; Y = S)] [62].

Cyclic voltammetry of the above dinuclear Cu(II) complexes in acetonitrile is characterised by two one-electron redox behaviour corresponding to Cu(II)/Cu(II) to Cu(II)/Cu(I) and Cu(II)/Cu(I) to Cu(I)/Cu(I) couples [62]. As expected, the redox potentials are dependent on the nature of the macrocyclic donors as well as on the type of bridging ligand present. As the number of 'soft' sulfur donors is increased in the series of azide bridged complexes: $[Cu_2L(N_3)]^{2+}$, where L = **38** (X, Y = NH), $[Cu_2L(N_3)]^{2+}$, where L = **38** (X = NH; Y = S), and $[Cu_2L(N_3)]^{2+}$, where L = **38** (X, Y = S), stabilisation of 'soft' Cu(I) is observed. This is reflected in a shift of the respective half-wave potentials to more positive values for each Cu(II)/Cu(II) → Cu(II)/Cu(I) couple ($E_{1/2} = -329$, -200 and $+211$ mV vs. NHE) and the corresponding Cu(II)/Cu(I) → Cu(I)/Cu(I) couple ($E_{1/2} = -549$, -449 and -41 mV vs. NHE). It is of interest to note the relative Cu(I) stabilisation that occurs for the azide bridged species $[Cu_2L(N_3)]^{2+}$, where L = **38** (X = NH; Y = S), ($E_{1/2} = -200$ mV and -449 mV) compared to the pyrazolide bridged $[Cu_2L(1H$-pyrazol-1-ide$)]^{2+}$, where L = **38** (X = NH; Y = S), ($E_{1/2} = -402$ and -635 mV).

The speciation of the mono- and di-Cu(II) complexes of **38** (X = NH; Y = S) has been investigated against pH values using spectrophotometric and potentiometric studies [63]. In the presence of 0.9 equivalents of Cu(II), the dominant species at pH < 6 is $[Cu(LH)]^{3+}$ ($\lambda_{max} = 637$ nm) — corresponding to protonation of the

secondary amine of the macrocyclic ring not involved in coordination to the Cu(II) ion. Between pH 6 and 11, the main species are $[CuL]^{2+}$ ($\lambda_{max} = 612$ nm) and $[Cu(LH_{-1})]^{+}$ ($\lambda_{max} = 602$ nm), while only at pH > 11 does the species $[Cu(LH_{-2})]$ exist in measurable concentrations. Formation of $[CuL]^{2+}$ from $[Cu(LH)]^{3+}$ ($pK_H = 6.33$) involves the deprotonation and concomitant coordination of the pyrazole group; $[CuL]^{2+}$ then undergoes deprotonation of its ammonium group and formation of a hydroxo species ($pK_H = 10.12$ and 10.76), the order of these two deprotonations being difficult to determine. The final product is of type $[Cu(LH_{-2})]$.

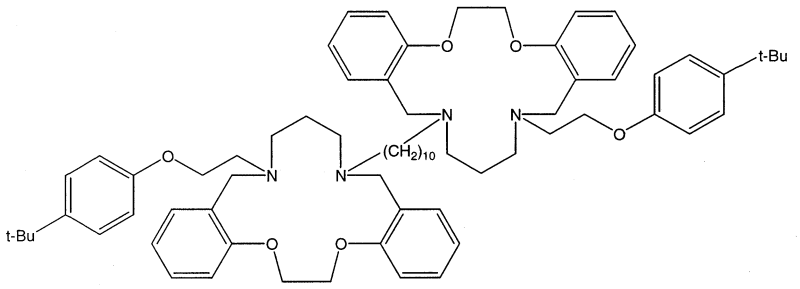

39

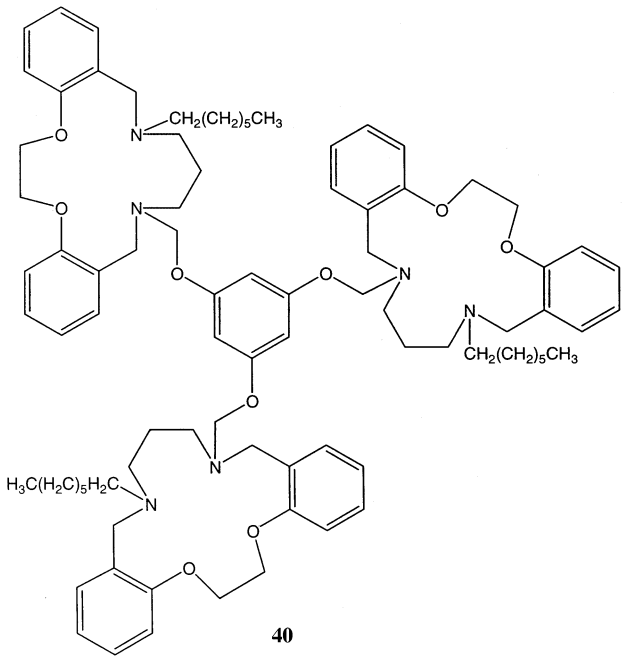

40

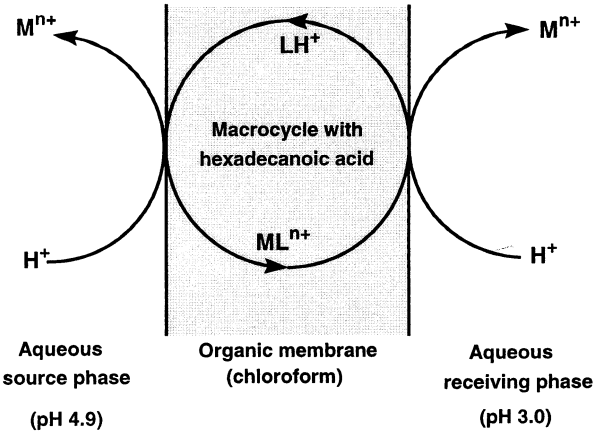

Fig. 11. The arrangement used for the transport of a metal ion across a chloroform membrane phase [68].

When the metal:ligand ratio is 1.8:1, $[Cu_2L]^{4+}$, L = **38** (X = NH; Y = S), is already formed at low pH. This species undergoes deprotonation of the pyrazole group ($pK_H = 2.41$) to form a new species in which the resulting pyrazolide group bridges the two Cu(II) centres ($\lambda_{max} = 627$ nm). The monohydroxo species $[Cu_2(LH_{-2})]^{2+}$ ($\lambda_{max} = 612$ nm) and dihydroxo species $[Cu_2(LH_{-3})]^{+}$ are also formed on two further deprotonations ($pK_H = 6.59$ and 11.71).

The binding of the bridging ligands N_3^-, pyrazole or 1*H*,1′*H*-4,4′-methanediyl-bispyrazole (bispyr) by the di-Cu(II) complex of **38** (X = NH; Y = S) to give ternary species, was investigated by means of spectrophotometric titration experiments. The results revealed that N_3^- and bispyr form both 1:1 and 2:1 ($[Cu_2L]^{3+}$:bridging ligand) species, whereas pyrazole only gives a 1:1 complex. Formation of the bispyr complexes was confirmed by electrospray mass spectrometry.

Our group has synthesised the di- and tri-linked macrocyclic systems incorporating N_2O_2-donor sets given by **39** and **40** as well as spiro-linked macrocycles incorporating N_2O_2- and N_3O_2-donor sets of type **41** ($n = 0$; R = H or $n = 1$; R = *t*-Bu), **42** [X = $(CH_2)_2$, $(CH_2)_3$ or $(CH_2)_2NH(CH_2)_2$] and **43** (R = H or *t*-Bu) [65–67]. Initial metal complexation studies involving the latter series of spiro-linked species indicated the formation of 2:1 (metal:ligand) complexes of Ni(II) and Cu(II) in solution. A series of competitive metal ion transport experiments (water–chloroform–water) have been performed in order to investigate structure–function relationships underlying the observed membrane transport behaviour. In these experiments the source phase contained equimolar concentrations (1.0×10^{-2} mol dm^{-3}) of Co(II), Ni(II), Cu(II), Zn(II), Cd(II), Ag(I) and Pb(II) while the membrane phase incorporated the ionophore (1×10^{-3} mol dm^{-3}) chosen from ligands of type **42** [X = $(CH_2)_2$ or $(CH_2)_3$] and **43** (R = H or *t*-Bu) together with hexadecanoic acid (4×10^{-3} mol dm^{-3}) [66]. A 'concentric cylinder' cell (Fig. 11), whose

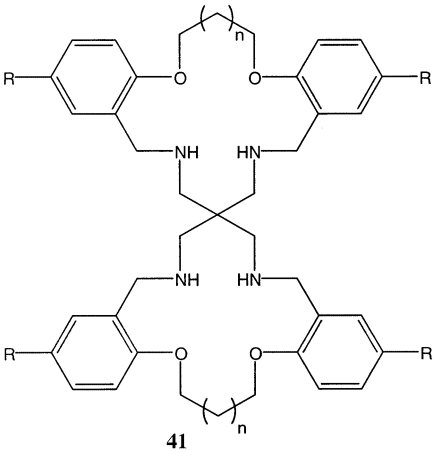

41

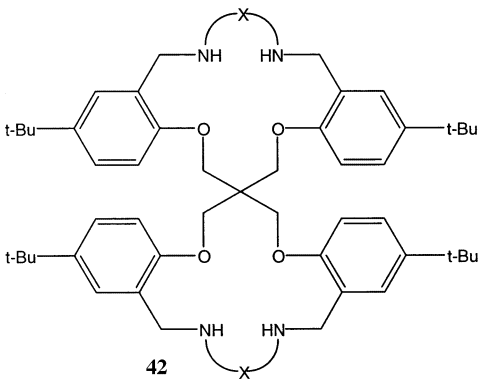

42

design had been described earlier [68], was employed for these experiments. The transport process was 'driven' by a back flux of protons, maintained by buffering the source and receiving phases at pH 4.9 and 3.0, respectively. Transport selectivity for Cu(II) was observed in all cases. In each case Ni(II) (between 13 and 20% of the total originally present in the source phase) was found to be present in the respective membrane phases after 24 h.

Comparison of the transport behaviour of **42** [$X = (CH_2)_2$] with an equivalent concentration of its single ring analogue reveals that the linked system results in a greater than threefold transport rate increase. However, for the system incorporating **42** [$X = (CH_2)_2$], the amount of Cu(II) remaining in the membrane phase, at 1%, is much smaller than found for the single ring system (46%). Thus, the effective transport behaviour for each of these systems is seen to be controlled by a subtle balance between metal uptake/metal loss into and out of the respective membrane phases.

In contrast to the behaviour of **42** [$X = (CH_2)_2$], comparison of the Cu(II) transport behaviour for **42** [$X = (CH_2)_3$] and its single ring analogue indicates that both are associated with quite moderate transport rates, with the single ring system yielding slightly higher transport efficiency ($J = 3.32 \times 10^{-7}$ mol h^{-1}) than an equivalent membrane concentration of the double ring system ($J = 2.23 \times 10^{-7}$ mol h^{-1}). For both systems, it seems that the overall lower J values are reflected by the small amount of Cu(II) present in the respective membrane phases after 24 h. This suggests that it is the passage of Cu(II) across the source phase/membrane phase interface that is inhibited in each of these systems, thus leading to lower overall transport rates.

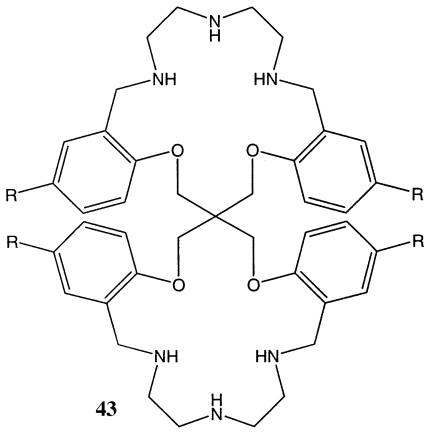

43

Finally, it is instructive to compare the transport results for the spiro-linked O_2N_3-donor ring derivatives **43** (R = H) and **43** (R = *t*-Bu). In the latter case the presence of *t*-butyl groups results in a drop in transport efficiency relative to the former system. While this is perhaps somewhat unexpected, the reason is apparent on inspection of the composition of the respective membrane phases after 24 h. Thus, the more lipophilic system yields enhanced extraction of Cu(II) into the membrane phase. However, once there, it is not so readily lost to the receiving phase relative to the system incorporating **43** (R = H); the result is a build up of Cu(II) in the membrane phase.

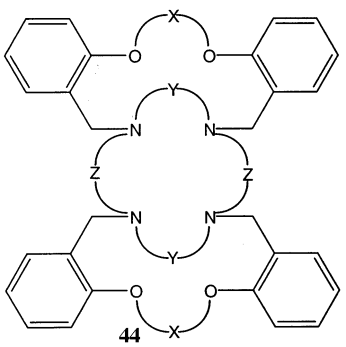

44

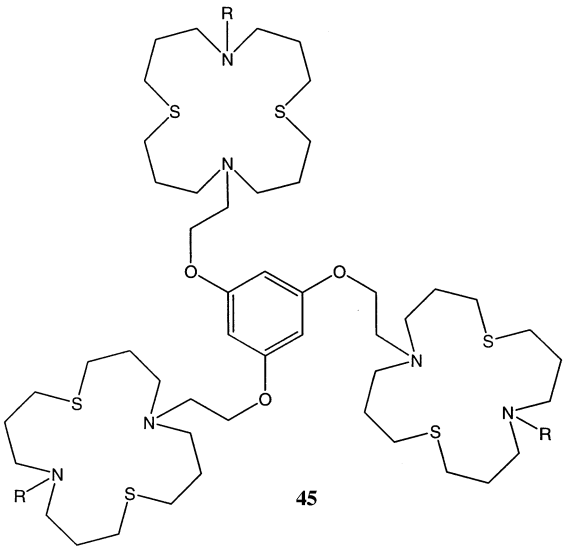

45

A new series of linked-ring, mixed oxygen–nitrogen donor systems of type **44** [X = $(CH_2)_2$, $(CH_2)_3$ or $(CH_2)_2O(CH_2)_2$; Y, Z = $(CH_2)_3$ and X = $(CH_2)_2O(CH_2)_2$; Y = $(CH_2)_2$; Z = $(CH_2)_3$] incorporating three macrocyclic cavities for use in transport studies related to those just discussed have recently been reported [69].

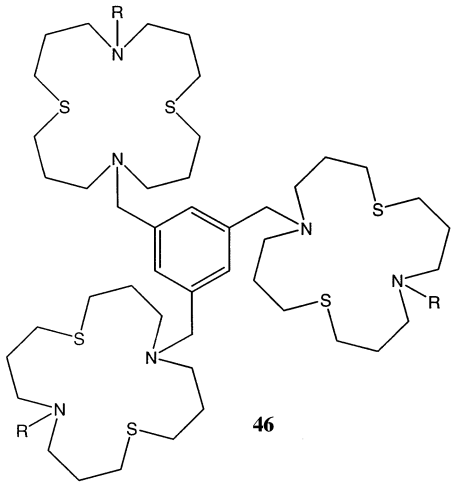

46

A strategy allowing the selective mono-*N*-protection of a 16-membered S_2N_2-donor macrocycle has enabled the construction of a number of tri-linked systems of type **45** (R = H or benzyl) and **46** (R = H or benzyl); in these, three macrocycles rings of the above type are connected to a 1,3,5-tribenzyl or a phloroglucinol core [70]. The trinuclear Cu(I), Pd(II) and Pt(II) complexes of both **45** (R = H) and **46** (R = H) have been isolated as their PF_6^- salts [71].

5. Linked heterotopic systems

Viable syntheses for obtaining the series of heteroditopic linked macrocycles given by **47** and **48** (X = $(CH_2)_2$, *m*-xylyl or *p*-xylyl; $n = 0$ or 1) have been developed using *N*-protected macrocyclic precursors and appropriate difunctional linking reagents [72]. A spectrophotometric titration experiment has been employed to demonstrate complexation of Cu(II) by **48** (X = *m*-xylyl; $n = 0$) in acetonitrile [73]. The results demonstrated the stepwise nature of Cu(II) uptake by this ligand. Thus, titration of the ligand in acetonitrile with $Cu(ClO_4)_2$ results in the appearance of a species ($\lambda_{max} = 525$ nm) which was postulated to correspond to the complexation of Cu(II) by the cyclam unit. This was followed by the formation of a second species ($\lambda_{max} = 610$ nm) assigned to the dinuclear species containing Cu(II) bound to both macrocyclic sites. Inspection of the LMCT bands associated with each process

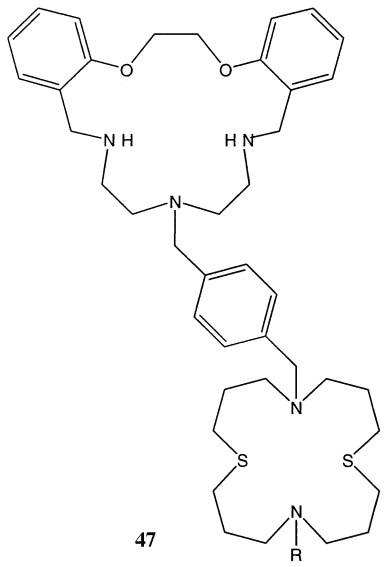

47

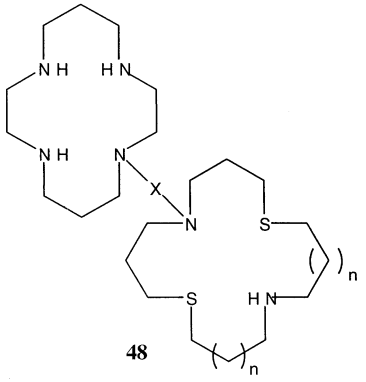

48

supported this hypothesis. $[Cu_2L](ClO_4)_4$, where L = **48** (X = *m*-xylyl; $n = 0$), has been isolated. Under the conditions employed the cyclic voltammogram of this complex in acetonitrile yielded two irreversible reduction waves ($E_{1/2} = -0.26$ and -0.50 V vs. Fc/Fc^+).

Acknowledgements

The authors acknowledge the support of the Australian Research Council.

References

[1] L.F. Lindoy, Coord. Chem. Rev. 174 (1998) 327.
[2] L.F. Lindoy, Adv. Inorg. Chem. 45 (1998) 75.
[3] L.F. Lindoy, Chemistry of Macrocyclic Ligand Complexes, Cambridge University Press, Cambridge, UK, 1989.
[4] M. Hiraoka (Ed.), Crown Ethers and Analogous Compounds — Studies in Organic Chemistry, vol. 45, Elsevier, Amsterdam, 1992, p. 335.
[5] J.S. Bradshaw, K.E. Krakowiak, R.M. Izatt, Aza-Crown Macrocycles, vol. 51, Wiley, New York, 1993.
[6] J.S. Bradshaw, R.M. Izatt, Z. Yan, Chem. Rev. 94 (1994) 939.
[7] J.P. Collman, P.S. Wagenknecht, J.E. Hutchison, Angew. Chem. Int. Ed. Engl. 33 (1994) 1537.
[8] L.F. Lindoy, I.M. Atkinson, Self-Assembly in Supramolecular Systems, The Royal Society of Chemistry, Cambridge, UK, 2000.
[9] J.-P. Sauvage (Ed.), Transition Metals in Supramolecular Chemistry, Wiley, New York, 1999.
[10] P.A. Vigato, S. Tamburini, D.E. Fenton, Coord. Chem. Rev. 106 (1990) 25.
[11] P. Guerrier, P.A. Vigato, D.E. Fenton, P.C. Hellier, Acta Chem. Scand. 46 (1992) 1025.
[12] R.W. Hay, J.R. Dilworth, K.B. Nolan (Eds.), Perspectives on Bioinorganic Chemistry, vol. 2, JAI Press, Greenwhich, CY, 1993, pp. 81–138.
[13] (a) E. De Clercq, N. Yamamto, R. Pawels, M. Baba, D. Schols, H. Nakashima, J. Balzarini, Z. Debyser, B.A. Murrer, D. Schwartz, D. Thornton, G. Bridger, S. Fricker, G. Henson, M. Abrams, D. Picker, Proc. Natl. Acad. Sci. USA 89 (1992) 5286. (b) G.J. Bridger, R.T. Skerlj, D. Thorhton, S. Padamanabhan, S.A. Martellucci, G.W. Henson, M.J. Abrams, N. Yamamoto, K. De Vreese, R. Pauwels, E. De Clercq, J. Med. Chem. 38 (1995) 366.
[14] (a) Y. Inouye, T. Kanomori, T. Yoshida, X. Bu, M. Shinoya, T. Koike, E. Kimura, Biol. Pharm. Bull. 17 (1994) 243. (b) Y. Inouye, T. Kanomori, M. Sugiyama, T. Yoshida, T. Koike, M. Shinoya, K. Enomoto, K. Suehiro, E. Kimura, Antiviral Chem. Chemother. 6 (1995) 337.
[15] (a) J. Dessolin, P. Vlieghe, J. Chermann, J. Kraus, J. Med. Chem. 42 (1999) 229. (b) G.J. Bridger, R.T. Skerlj, S. Padmanabhan, S.A. Martellucci, G.W. Henson, S. Struyf, M. Witvrouw, D. Schols, E. De Clercq, J. Med. Chem. 42 (1999) 3971. (c) J.A. Este, C. Cabrera, E. De Clercq, S. Struyf, J. Van Damme, G.J. Bridger, R.T. Skerlj, M.J. Abrams, G.W. Henson, A. Gutierrez, B. Clotet, D. Schols, Mol. Pharm. 55 (1999) 67.
[16] (a) R. Garg, S.P. Gupta, H. Gao, M.S. Babu, A.K. Debnath, C. Hansch, Chem. Rev. 99 (1999) 3525. (b) E. Kimura, T. Koike, Y. Inoue, in: R.W. Hay, J.R. Dilworth, K.B. Nolan (Eds.), Perspective on Bioinorganic Chemistry, vol. 4, JAI Press, Greenwhich, CT, 1999, pp. 145–164. (c) G.J. Bridger, R.T. Skerly, Advances in Antiviral Drug Design, vol. 3, JAI Press, Greenwhich, CT, 1999, pp. 161–229.
[17] N. Tanaka, Y. Kobayashi, S. Takamoto, Chem. Lett. (1977) 107.

[18] L.J. Farrugia, P.A. Lovatt, R.D. Peacock, J. Chem. Soc. Dalton Trans. (1997) 911.
[19] B. Graham, G.D. Fallon, M.T.W. Hearn, D.C.R. Hockless, G. Lazarev, L. Spiccia, Inorg. Chem. 36 (1997) 6366.
[20] See, for example, refs. in: W.B. Tolman, Acc. Chem. Res. 30 (1997) 227.
[21] S. Mahapatra, S. Kaderli, A. Llobet, Y.-M. Neuhold, T. Palanché, J.A. Halfen, V.G. Young Jr, T.A. Kaden, L. Que Jr, A.D. Zuberbühler, W.B. Tolman, Inorg. Chem. 36 (1997) 6343.
[22] S. Mahapatra, V.G. Young Jr, S. Kaderli, A.D. Zuberbühler, W.B. Tolman, Angew. Chem. Int. Ed. Engl. 36 (1997) 130.
[23] M.D. Snodin, P.D. Beer, M.G.B. Drew, J. Chem. Soc. Dalton Trans. (1997) 3407.
[24] P.D. Beer, M.G.B. Drew, P.B. Leeson, K. Lyssenko, M.I. Ogden, J. Chem. Soc. Chem. Commun. (1995), 929.
[25] W.H. Chapman Jr, R. Breslow, J. Am. Chem. Soc. 117 (1995) 5462.
[26] F.H. Fry, B. Graham, L. Spiccia, D.C.R. Hockless, E.R.T. Tiekink, J. Chem. Soc. Dalton Trans. (1997) 827.
[27] S.J. Brudenell, L. Spiccia, A.M. Bond, G.D. Fallon, D.C.R. Hockless, G. Lazarev, P.J. Mahon, E.R.T. Tiekink, Inorg. Chem. 39 (2000) 881.
[28] L. Spiccia, G.D. Fallon, M.J. Grannas, P.J. Nichols, E.R.T. Tiekink, Inorg. Chim. Acta 279 (1998) 192.
[29] S.J. Brudenell, L. Spiccia, A.M. Bond, P.C. Mahon, D.C.R. Hockless, J. Chem. Soc. Dalton Trans. (1998) 3919.
[30] (a) S.J. Brudenell, L. Spiccia, E.R.T. Tiekink, Inorg. Chem. 35 (1996) 1974. (b) S.J. Brudenell, L. Spiccia, A.M. Bond, P. Comba,, D.C.R. Hockless, Inorg. Chem. 37 (1998) 3705.
[31] S.J. Brudenell, L. Spiccia, D.C.R. Hockless, E.R.T. Tiekink, J. Chem. Soc. Dalton Trans. (1999) 1475.
[32] L. Spiccia, B. Graham, M.T.W. Hearn, G. Lazarev, B. Moubaraki, K.S. Murray, E.R.T. Tiekink, J. Chem. Soc. Dalton Trans. (1997) 4089.
[33] B. Graham, M.J. Grannas, M.T.W. Hearn, C.M. Kepert, L. Spiccia, B.W. Skelton, A.H. White, Inorg. Chem. 39 (2000) 1092.
[34] P.D. Beer, D. Gao, J. Chem. Soc. Chem. Commun. (2000) 443.
[35] M.I. Burguete, E. García-España, S.V. Luis, J.F. Mirvet, L. Payá, M. Querol, C. Soriano, J. Chem. Soc. Chem. Commun. (1998) 1823.
[36] P.V. Bernhardt, L.A. Jones, J. Chem. Soc. Chem. Commun. (1997), 655.
[37] T.A. Khan, M.A. Rather, N. Jahan, S.P. Varkey, M. Shakir, Synth. React. Inorg. Met.-Org. Chem. 27 (1997) 843.
[38] K.V. Gobi, T. Ohsaka, Electrochim. Acta 44 (1998) 269.
[39] T. Koike, M. Takashige, E. Kimura, H. Fujioka, M. Shiro, Chem. Eur. J. 2 (1996) 617.
[40] H. Fujioka, T. Koike, N. Yamada, E. Kimura, Heterocycles 42 (1996) 775.
[41] E. Kimura, S. Aoki, T. Koike, M. Shiro, J. Am. Chem. Soc. 119 (1997) 3068.
[42] E. Kimura, M. Kikuchi, H. Kitamura, T. Koike, Chem. Eur. J. 5 (1999) 3113.
[43] S. Aoki, E. Kimura, J. Am. Chem. Soc. 122 (2000) 4542.
[44] S. Sun, J. Saltmarsh, S. Mallik, K. Thomasson, J. Chem. Soc. Chem. Commun. (1998) 519.
[45] Y. Dong, L.F. Lindoy, G. Wei, Unpublished work.
[46] P.V. Bernhardt, E.J. Hayes, J. Chem. Soc. Dalton Trans. (1998) 3539.
[47] A. Damsyik, P.J. Davies, C.I. Keeble, M.R. Taylor, K.P. Wainwright, J. Chem. Soc. Dalton Trans. (1998) 703.
[48] S.-G. Kang, K. Ryu, M.P. Suh, J.H. Jeong, Inorg. Chem. 36 (1997) 2478.
[49] M. Lachkar, B. Andrioletti, B. Boitrel, R. Guilard, A. Atmani, New J. Chem. 19 (1995) 777.
[50] F. Rabiet, F. Denat, R. Guilard, Synth. Commun. 27 (1997) 979.
[51] S. Brandes, F. Denat, S. Lacour, F. Rabiet, F. Barbette, P. Pullumbi, R. Guilard, Eur. J. Org. Chem. (1998) 2349.
[52] M. Lachkar, R. Guilard, A. Atmani, A. De Cian, J. Fischer, R. Weiss, Inorg. Chem. 37 (1998) 1575.
[53] Y. Gok, H. Kantekin, Polyhedron 16 (1997) 2413.
[54] Y. Gok, H. Kantekin, Acta Chem. Scand. 51 (1997) 664.

[55] (a) G.N. Schrauzer, Chem. Ber. 95 (1962) 1438. (b) F. Umland, D. Thierig, Angew. Chem. 74 (1962) 388.
[56] Y. Gok, H. Kantekin, New J. Chem. 19 (1995) 461.
[57] Y. Gok, S. Karaböcek, N. Karaböcek, Y. Atalay, New J. Chem. 19 (1995) 1275.
[58] Y. Gok, S. Karaböcek, M.N. Misir, Transition Met. Chem. 21 (1996) 331.
[59] Y. Gok, Polyhedron 15 (1996) 1355.
[60] Y. Gok, Polyhedron 15 (1996) 3933.
[61] L. Behle, M. Neuburger, M. Zehnder, T.A. Kaden, Helv. Chim. Acta 78 (1995) 693.
[62] H. Weller, L. Siegfried, M. Neuburger, M. Zehnder, T.A. Kaden, Helv. Chim. Acta 80 (1997) 2315.
[63] H. Weller, T.A. Kaden, G. Hopfgartner, Polyhedron 17 (1998) 4543.
[64] T.A. Kaden, Coord. Chem. Rev. 190-192 (1999) 371.
[65] I.M. Atkinson, D.M. Boghai, B. Ghanbari, L.F. Lindoy, G.V. Meehan, V. Saini, Aust. J. Chem. 52 (1999) 351.
[66] J. Kim, L.F. Lindoy, O.A. Matthews, G.V. Meehan, J. Nachbaur, V. Saini, Aust. J. Chem. 48 (1995) 1917.
[67] J. Kim, A.J. Leong, L.F. Lindoy, J. Nachbaur, A. Nezhadali, G. Rounaghi, G. Wei, J. Chem. Soc. Dalton Trans. (2000) 3453.
[68] P.S.K. Chia, L.F. Lindoy, G.W. Walker, G.W. Everett, Pure and Appl. Chem. 65 (1993) 521.
[69] T.-H. Ahn, J. Kim, L.F. Lindoy, J. Wang, Aust. J. Chem. 52 (1999) 1139.
[70] A.M. Groth, L.F. Lindoy, G.V. Meehan, J. Chem. Soc. Perkin Trans. 1 (1996) 1553.
[71] I.M. Atkinson, A.M. Groth, L.F. Lindoy, M.P. Lowe, G.V. Meehan, Unpublished work.
[72] J.D. Chartres, A.M. Groth, L.F. Lindoy, M.P. Lowe, G.V. Meehan, Perkin Trans. 1 (2000) 3444.
[73] J.D. Chartres, L.F. Lindoy, G.V. Meehan, Unpublished work.